(2)

NAVAL POSTGRADUATE SCHOOL

Monterey, California

THESIS

EXPLORATORY EXPERIMENTAL INVESTIGATION OF A WAVE PROPELLER

by

Carl W. Dane

March, 1992

Thesis Advisor: Max F. Platzer
Co-Advisor: S. K. Hebbar

Approved for public release; distribution is unlimited

REPORT DOCUMENTATION PAGE

1a. REPORT SECURITY CLASSIFICATION UNCLASSIFIED	1b. RESTRICTIVE MARKINGS
2a. SECURITY CLASSIFICATION AUTHORITY	3. DISTRIBUTION/AVAILABILITY OF REPORT Approved for public release; distribution is unlimited.
2b. DECLASSIFICATION/DOWNGRADING SCHEDULE	
4. PERFORMING ORGANIZATION REPORT NUMBER(S)	5. MONITORING ORGANIZATION REPORT NUMBER(S)
6a. NAME OF PERFORMING ORGANIZATION Naval Postgraduate School 6b. OFFICE SYMBOL (*If applicable*) AA/PL	7a. NAME OF MONITORING ORGANIZATION Naval Postgraduate School
6c. ADDRESS (*City, State, and ZIP Code*) Monterey, CA 93943-5000	7b. ADDRESS (*City, State, and ZIP Code*) Monterey, CA 93943-5000
8a. NAME OF FUNDING/SPONSORING ORGANIZATION 8b. OFFICE SYMBOL (*If applicable*)	9. PROCUREMENT INSTRUMENT IDENTIFICATION NUMBER
8c. ADDRESS (*City, State, and ZIP Code*)	10. SOURCE OF FUNDING NUMBERS Program Element No / Project No / Task No / Work Unit Accession Number

11. TITLE (*Include Security Classification*)
EXPLORATIORY EXPERIMENTAL INVESTIGATION OF A WAVE PROPELLER

12. PERSONAL AUTHOR(S) Carl W. Dane

13a. TYPE OF REPORT	13b. TIME COVERED	14. DATE OF REPORT (*year, month, day*)	15. PAGE COUNT
Master's Thesis	From To	1992, March	68

16. SUPPLEMENTARY NOTATION
The views expressed in this thesis are those of the author and do not reflect the official policy or position of the Department of Defense or the U.S. Government.

17. COSATI CODES			18. SUBJECT TERMS (*continue on reverse if necessary and identify by block number*)
FIELD	GROUP	SUBGROUP	Usnsteady Excitation, Katzmayr effect, high lift

19. ABSTRACT (*continue on reverse if necessary and identify by block number*)

A low-speed wind tunnel investigation was conducted to determine if a small secondary airfoil, or wave propeller, oscillating in a rotary plunging motion, could significantly affect the airflow over a lifting airfoil surface enough to delay the onset of stall. The lifting airfoi shape was a NACA 66(215)-216, chosen for it's chordwise pressure port instrumentation. Testing consisted of measruring the pressure distribution of the NACA 66(215)-216 airfoil past the stall angle-of-attack, and then again in combination with the wave propeller. The wave propeller was located in two different positions; above the lifting airfoils trailing edge, and aft of the trailing edge. The propeller was operated in both colckwise and counter-clockwisse directions. The propeller effectiveness was evaluated by comparing the pressure distributions and computed lift curve slopes with and without propeller operation. Reynolds number vaired from 1.28×10^5 to 2.56×10^5. Mechanical limitations resulted in testing to only ten percent of the desired wave propeller speeds. Results indicated that the wave propeller acted to block the air flow over the lifting wing causing early separation and loss of lift.

20. DISTRIBUTION/AVAILABILITY OF ABSTRACT	21. ABSTRACT SECURITY CLASSIFICATION	
☒ UNCLASSIFIED/UNLIMITED ☐ SAME AS REPORT ☐ DTIC USERS	UNCLASSIFIED	
22a. NAME OF RESPONSIBLE INDIVIDUAL Max F. Platzer	22b. TELEPHONE (*Include Area code*) (408) 646-2058	22c. OFFICE SYMBOL AA/PL

DD FORM 1473, 84 MAR — 83 APR edition may be used until exhausted. All other editions are obsolete.

Approved for public release; distribution is unlimited.

Exploratory Experimental Investigation of a Wave Propeller

by

Carl W. Dane
B.S., California State Polytechnic University, 1983
of Pomona

Submitted in partial fulfillment
of the requirements for the degree of

MASTER OF SCIENCE IN AERONAUTICAL ENGINEERING

from the

NAVAL POSTGRADUATE SCHOOL
March 1992

Author: _____
Carl W. Dane

Approved by: _____
Max F. Platzer, Thesis Advisor

_____
S. K. Hebbar, Co-Advisor

_____
Daniel J. Collins, Chairman
Department of Aeronautics and Astronautics

ABSTRACT

A low-speed wind tunnel investigation was conducted to determine if a small secondary airfoil, or wave propeller, oscillating in a rotary plunging motion, could significantly affect the airflow over a lifting airfoil surface enough to delay the onset of stall. The lifting airfoil shape was a NACA 66(215)-216, chosen for it's chordwise pressure port instrumentation. Testing consisted of measuring the pressure distribution of the NACA 66(215)-216 airfoil past the stall angle-of-attack, and then again in combination with the wave propeller. The wave propeller was located in two different positions; above the lifting airfoil's trailing edge, and aft of the trailing edge. The propeller was operated in both clockwise and counter-clockwise directions. The propeller effectiveness was evaluated by comparing the pressure distributions and computed lift curve slopes with and without propeller operation. Reynolds number varied from 1.4×10^5 to 2.57×10^5. Mechanical limitations resulted in testing to only ten percent of the desired wave propeller speeds. Results indicated that the wave propeller acted to block the air flow over the lifting wing causing early separation and loss of lift.

TABLE OF CONTENTS

LIST OF FIGURES

LIST OF SYMBOLS AND ABBREVIATIONS

ccw	Counter-clockwise
cw	Clockwise
deg	degrees
fps	feet per second
NACA	National Advisory Committee For Aeronautics
r	Propeller radius of rotation (feet)
Re	Reynolds Number
RPM	Revolutions Per Minute
U	Wave Propeller rotational speed (fps)
V	Wind tunnel free-stream velocity (fps)
α	Angle-of-attack for NACA 66(215)-216 airfoil (deg)
β	Angle-of-attack for Schmidt's aft wing (deg)
ε	Angle-of-attack for Wave Propeller (deg)
λ	Ratio of propeller speed to free-stream velocity
Ω	Propeller rotational rate (RPM)

ACKNOWLEDGMENT

My thanks go out to Dr. Platzer and Dr. Hebbar. Their encouragement and guiding hands were appreciated. Credit is due to Mr. Jack King and Mr. John Moulton. Without their expertise and timely help this project would never have been accomplished.

I want to thank my wife, Jody, for the tremendous sacrifices she made in bearing our first child and becoming a "single parent" while I went off to school. And to my daughter Channing, a special thanks for the weekend smiles she gave that kept my sanity intact throughout a fast paced year of academia.

I. INTRODUCTION

Experimental research to enhance lift at post-stall angles-of-attack has long been an item of interest. Many methods have been examined to delay airfoil stall. Such methods traditionally included steady-state boundary layer control through continuous suction or blowing and flow control by use of slat and flap geometry. Stall delay has also been attempted through the use of unsteady excitation mechanisms. A recent review of this area of research was published in the Progress In Aerospace Sciences [Ref. 1].

The topic of this thesis is another unsteady flow excitation device which seems to be virtually unknown in the United States. It is the wave propeller first suggested by Wilhelm Schmidt of the Technical University of Dresden, Germany. His experimentation was conducted from 1940 through 1965 and was reported on in the German Journal of Flight Sciences in 1965 [Ref. 2].

Schmidt's wave propeller consisted of a single airfoil mounted off center between two circular plates which rotated about their centroid. In motion, the wave propeller performed a plunging or flapping motion which was perpendicular to the airflow. This physical phenomenon, commonly known as the "Katzmayr effect", was mathematically shown by Garrick to produce a net propulsive force [Ref. 3]. It is noteworthy to

recall that birds derive their propulsive forces from the Katzmayr effect.

Schmidt mounted his wave propeller in parallel aft of a large lifting wing surface and made lift measurements. The ratio of the wave propeller rotational velocity (U) to the free stream velocity (V) (a parameter defined as λ) was a primary test consideration. Schmidt also varied the location and angle-of-attack of the wave propeller (ε) with respect to the free-stream. Furthermore, he mounted a smaller stationary wing aft of the wave propeller set at various angles-of-attack (β), and showed that such an arrangement doubled the propulsive efficiency. A reproduction of Schmidt's results is shown in Figure 1.

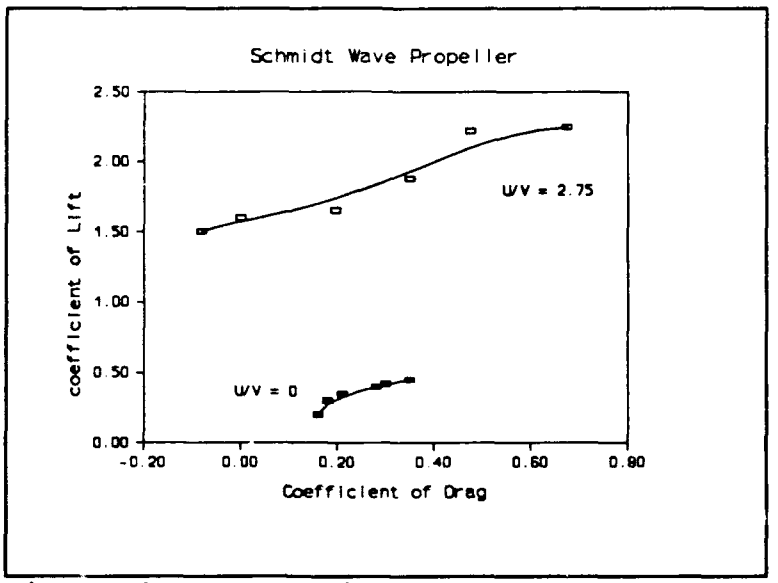

Figure 1. Schmidt's Wave Propeller Results

Results from Schmidt's work indicate that with the appropriate conditions (λ = 2.75, ε = 10 degrees, β = 45 degrees) the steady-state stall angle-of-attack (α) could be increased to beyond 25 degrees. A corresponding lift coefficient increase of almost four times the steady state value was also realized.

The research reported in the following sections was undertaken in an attempt to verify Schmidt's results, determine parameters for optimum propeller performance in propulsive force and increased lift, and obtain a better physical understanding of the aerodynamics of the wave propeller.

II. EXPERIMENTAL SET-UP

A. TEST EQUIPMENT

The test data presented in this paper were gathered in the Naval Postgraduate School low speed wind tunnel [Ref. 4]. A computer automated data acquisition system was used to obtain the pressure data over a NACA 66(215)-216 airfoil. The wind tunnel and the data acquisition system are described in Appendix A. The computer programs used to process the pressure data are described in Appendix B. The NACA 66(215)-216 airfoil was chosen as the primary lifting surface for its readily available instrumentation. The lifting airfoil chord was 12 inches, and the span of 28 inches spanned the wind tunnel test section. The lifting airfoil could be set between zero and 20 degrees angle-of-attack (α).

Time constraints for the purchase or fabrication of equipment that comprised the wave propeller and its drive mechanism resulted in some innovative (if undesirable) design decisions. A section of extruded tubing in an airfoil shape was used for the wave propeller (Figure 2). Figure 2 only approximates the propeller shape. The actual tubing used had a smooth contour.

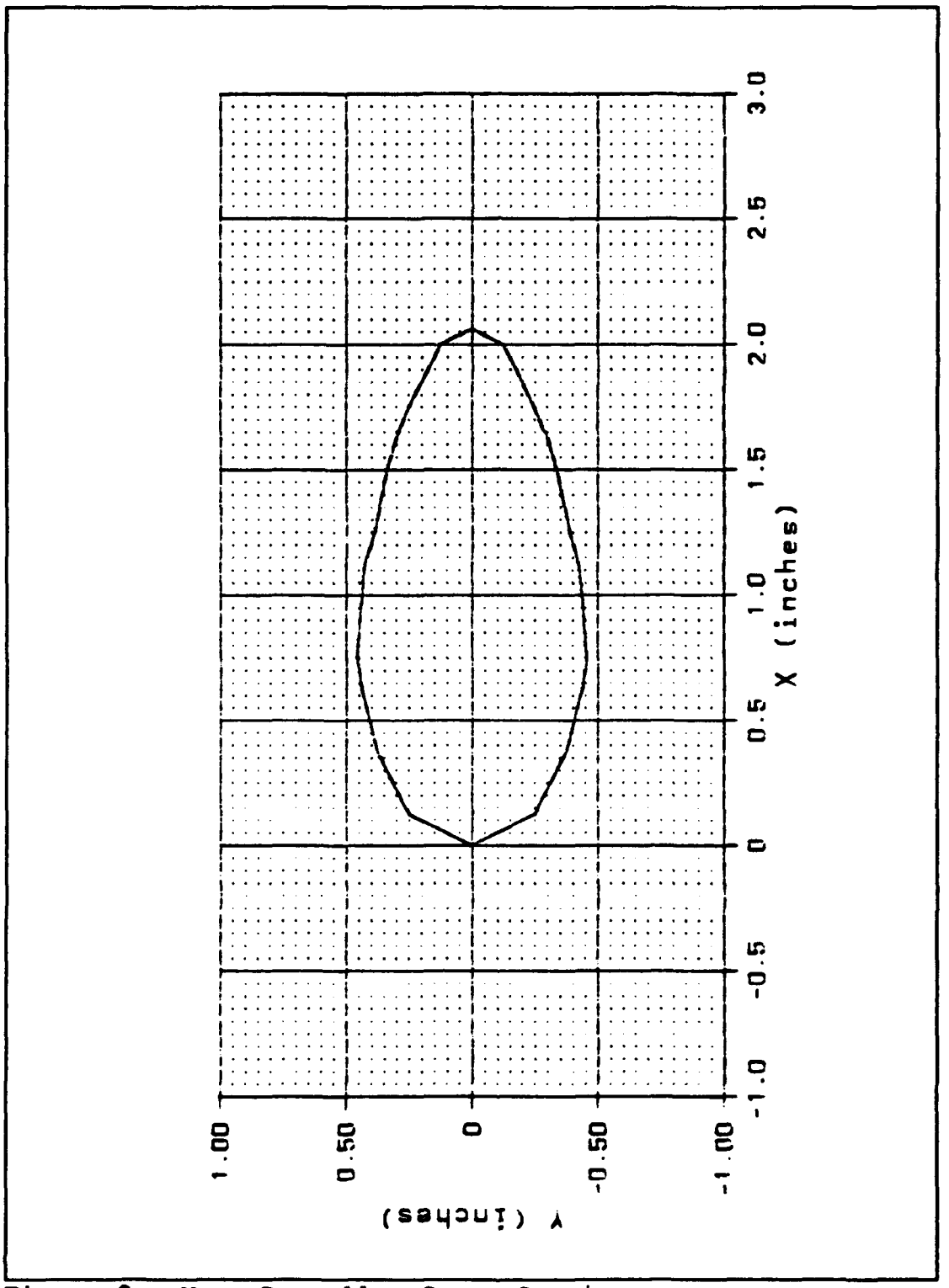

Figure 2. Wave Propeller Cross Section

The tubing approximated a symmetric airfoil of 2 1/16 inch chord and 44 percent thickness. One end of the wave propeller was attached to a sprocket which was driven by a direct current motor. A second sprocket, chain driven off the first sprocket, was linked to the propeller's trailing edge in such a manner that the propeller's angle-of-attack with respect to the free-stream was maintained as it moved. The complete drive mechanism was mounted to a stand which rested on the top of the tunnel test section. Cutouts in the tunnel roof allowed the wave propeller to be extended into the test section. Figures 3 and 4 show the wave propeller mechanism in place.

A bottom mount component was initially installed for the wave propeller. The lower end of the propeller extended into a plate which rotated about a bearing. The motor driven sprocket was to provide the drive force, with the lower end acting as a second anchor point, but free to rotate with the driving sprocket. Wobble in the lower bearings, however, resulted in excessive binding due to phase lags between the wave propeller's upper and lower attachment points. Therefore, the bottom mount was removed and the upper mount was reinforced.

The ball joint linkage used to connect the propeller's trailing edge to the aft sprocket also failed to operate

Figure 3. Wave Propeller

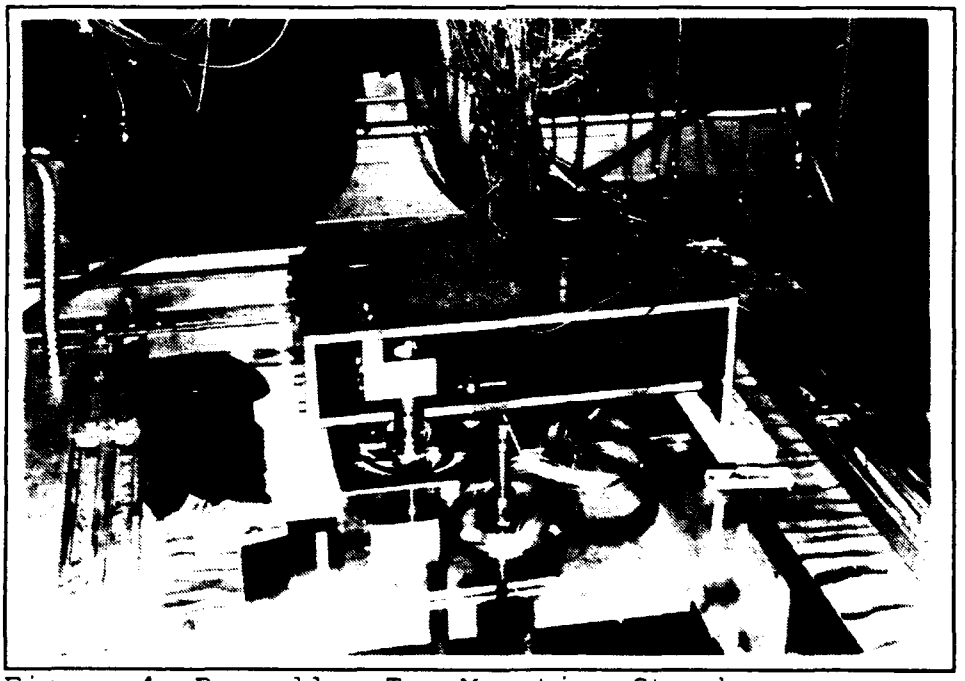

Figure 4. Propeller Top Mounting Stand

B. TEST PROCEDURE

Testing was performed for two different wave propeller locations. The locations are shown in Figures 5 and 6. The coordinate system origin was located at the lifting wing's pivot point (0.5 chord), with positive x being towards the trailing edge, and positive y towards the upper surface. Propeller motion was defined clockwise (cw) or counter-clockwise (ccw) as observed from above.

The propeller was located and the mount was fixed in position using safety wire. A direction of motion and tunnel velocity was set and the wave propeller was started. The propeller was always run at its maximum speed. Since the propeller was not mounted to the angle-of-attack turn table, the lifting airfoil's trailing edge moved away from the propeller as angle-of-attack was increased. Propeller speed was determined by a strobe light located above the test section and next to the mounting stand.

Pressure data on the lifting airfoil was recorded for angles-of-attack from 20 down to zero degrees. This was repeated for each tunnel velocity and propeller direction. Lift curves and drag polars were developed by integration of the pressure data.

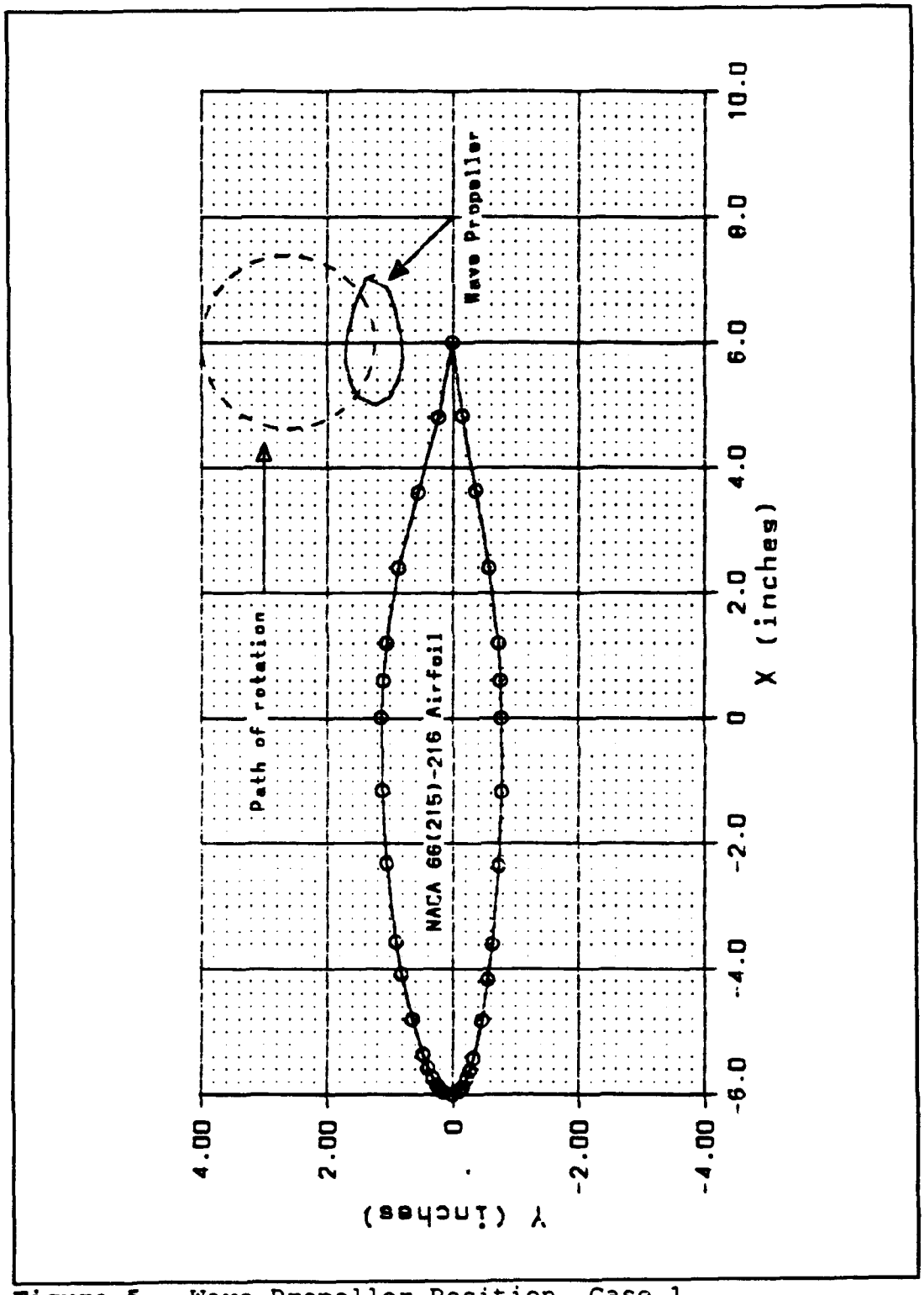

Figure 5. Wave Propeller Position, Case 1

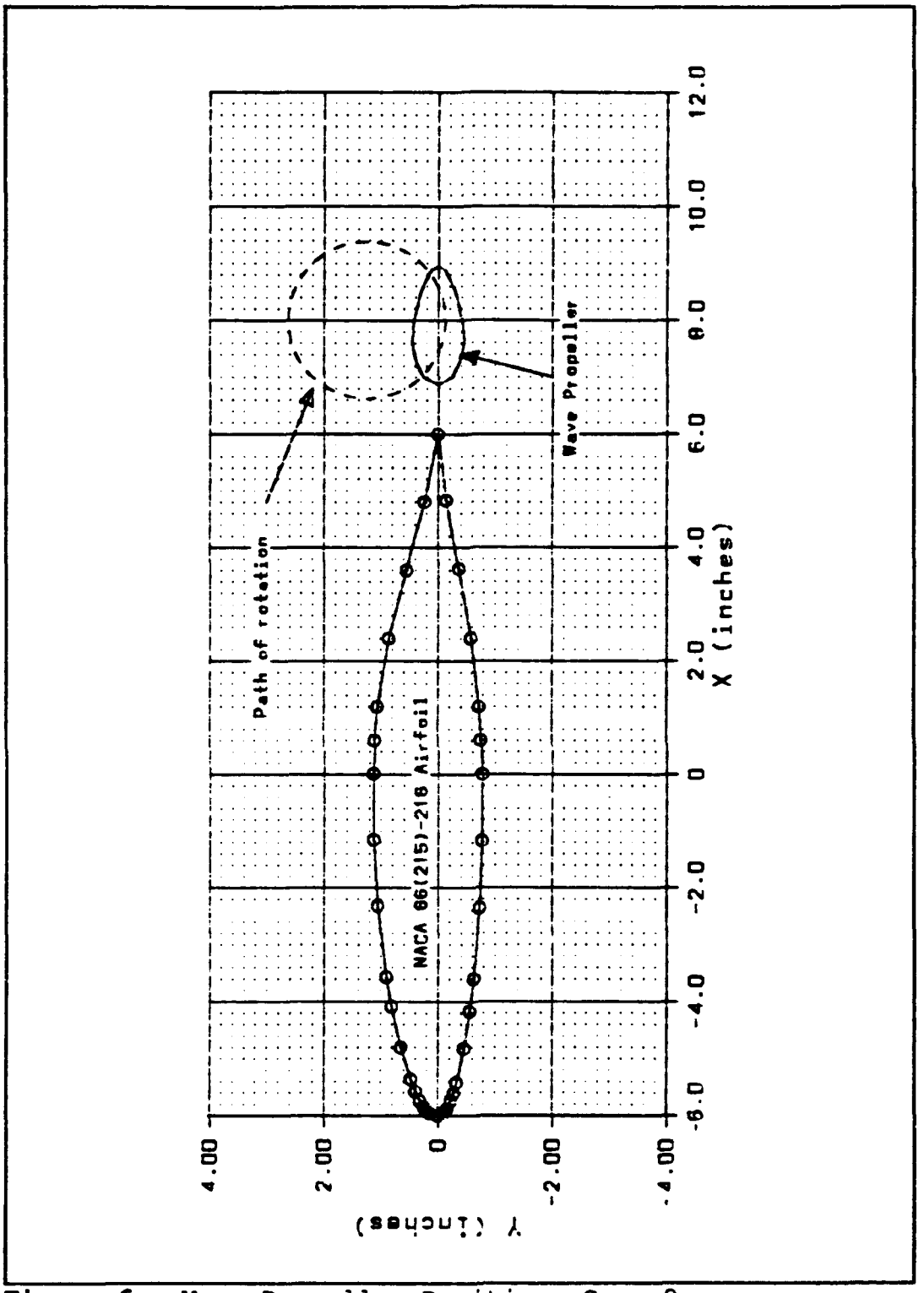

Figure 6. Wave Propeller Position, Case 2

III. RESULTS

The test data is displayed in Appendix C. Pressure distributions and calculated lift curves are shown for the NACA 66(215)-216 airfoil alone, and with the propeller present and operating.

A. NACA AIRFOIL

Test data was initially gathered on the NACA 66(215)-216 in the absence of the propeller. Figure 7 shows a comparison between pressure distribution test data at two different Reynolds numbers. The effects of low Reynolds Number can be seen in the lower suction peak and increased pressure across the forward half of the upper surface. The deviation in the pressure coefficient from 50 to 70 percent chord is due to the unsteady boundary layer separation.

Pressure distributions for selected angles-of-attack are shown in Figures 8 through 10. These figures include data for tunnel speeds of 30, 60, and 130 feet per second. Low Reynolds Number effects can again be seen. Pressure distributions for tunnel speeds at and above 130 feet per second were similar and are not included.

Figure 11 shows the measured lift curves for the test data as a function of Reynolds Number. Boundary layer separation began at approximately 13 degrees and was fully separated by

18 degrees angle-of-attack. Thus stall for the NACA 66(215)-216 airfoil was determined to occur at between 15 and 16 degrees angle-of-attack. This agrees with published results for a NACA 66-215 airfoil [Ref 5.].

B. WAVE PROPELLER

Data for the wave propeller tests are shown in Figures 12 through 41. Test conditions for λ values of 0.16, 0.22 and 0.33 were evaluated. In all tests, the presence of the wave propeller acted to block flow over the lifting airfoil's surface. This caused early separation and loss of lift.

Figures 12 through 32 include pressure distributions and measured lift curves for the propeller located as defined by Case 1. Propeller operation in the cw direction had a greater detrimental effect on the pressure distribution than operation in the ccw direction. The entrainment of air due the propeller's motion may have offset the effect of the propeller's blockage of the airflow during counter-clockwise operation.

Figures 33 through 39 include the pressure distributions and lift curves for the propeller location defined by Case 2. In this position, propeller direction made no difference in the results. Air flow was blocked and lift was reduced.

The lift data presented was not corrected for fluctuations in the tunnel speed. Free-stream velocities could vary as much as two feet per second from the target speed for each

angle-of-attack. Changes from the target free-stream velocities propagated as errors into the lift calculations. Lift and pressure coefficients are both functions of the tunnel dynamic pressure. Dynamic pressure is essentially velocity squared. Thus error propagated into the lift curve as a function of change from the target velocity squared.

The automated data collection system would continue incrementing the test α and recording data until the 2 foot per second velocity window was exceeded. At that point the operator would be notified to adjust the tunnel back to the target speed. Speed changes could affect the calculated lift coefficients by as much as 9.75%, 12.9% and 19% low, to 10.25%, 13.8%, and 21% high for targeted speeds of 40, 30, and 20 feet per second respectively. This partially accounts for the dramatic changes in lift coefficients for a given test condition.

IV. CONCLUSIONS AND RECOMMENDATIONS

A. CONCLUSIONS

Schmidt's wave propeller results could not be verified. The propeller speeds could not be reached to match the conditions reported by Schmidt, which were approximately ten times the speeds attained in this report. Furthermore, propeller location was limited by the physical dimensions of the wind tunnel, and incorporation of the aft stationary wing used by Schmidt was not accomplished.

The effectiveness of the wave propeller is dependent upon:

- Speed of operation
- Location of propeller with respect to the lifting wing
- Angle-of-attack of the propeller
- Presence or absence of the aft located stationary wing and its angle-of-attack

Each of these parameters must be accounted for to determine the optimum configuration for a wave propeller system.

B. RECOMMENDATIONS

The failure to meet the objectives of this thesis was attributed to the inability of the wave propeller drive mechanism to attain the desired test conditions. Numerous changes must be made to the current design to attain the required test conditions.

The current motor must be replaced with one capable of at least a three horse power output. This will be required to reach the λ values reported by Schmidt.

The chain drive mechanism should be replaced with a smoother operating system. A pulley drive system that anchors the wave propeller at each end should be investigated.

An accurate way to maintain the wave propeller angle-of-attack, ε, at other than zero degrees must be incorporated. Additionally, the wave propeller should be required to maintain its position relative to the lifting airfoil as the lifting airfoil's angle-of-attack is changed.

A location for the testing other than the low speed wind tunnel should be considered. There is insufficient space in the tunnel test section to allow for significant variation between the relative positions of the propeller and the lifting airfoil. The wave propeller system should also include Schmidt's stationary airfoil aft of the propeller. This will be required to determine the optimum propeller performance parameters.

APPENDIX A

The Naval Postgraduate School low speed wind tunnel was designed by the Aerolab Development Company of Pasadena, California. The tunnel is a single-return tunnel, 64 feet long, and between 21.5 and 25.5 feet wide. It is powered by a 100 horse power electric motor, driving a three bladed variable pitch fan through a four speed International truck transmission. Directly downstream of the fan is a set of eight stator blades to remove the swirl imparted by the fan blades.

Turning vanes are installed in each of the four 90-degree bends. The vanes consist of plane curved sheets with segmented trailing edges for precise flow adjustment. After passing through three 90-degree turns the flow enters the settling chamber.

The settling chamber contains two turbulence screens. The screens are made from fine wire and are placed approximately six inches apart. Turbulent fluctuations are broken down into small low energy fluctuations that are eventually dissipated as heat.

After exiting the settling chamber the flow enters the contraction cone. The contraction cone smoothly accelerates to the speeds desired in the test section.

The test section cross-sectional area is 8.75 square feet, or approximately one tenth of the settling chamber area. The test section is rectangular with glass corner fillets through which illumination is provided. The walls are slightly divergent to offset boundary layer growth. Hinged windows on either side permit access and viewing of the test section. A reflection plane is mounted on the test section floor to contain portions of a force balance and angle-of-attack drive equipment. The available area for mounting models is 28 1/4 inches high, and 40 7/8 inches wide.

The tunnel test section was designed to operate at atmospheric pressure. Since leakage occurs throughout the low velocity high pressure portions of the tunnel, a breather slot is located just aft of the test section. The slot extends around the exterior of the tunnel and allows external air to flow into the tunnel and make up leakage losses. This ensures that the test section maintains a uniform pressure throughout operation.

A gradual widening diffusing duct is placed behind the test section to convert the high velocity flow kinetic energy back into pressure energy. A heavy wire screen is located in the diffuser to protect the downstream turning vanes and driving fan from damage due to loose equipment breaking free during operation.

Four static pressure taps and a temperature probe are located downstream of the turbulence screens in the settling

chamber. Four more static pressure taps are located just forward of the test section in the contraction cone. The static ports are connected to a water manometer and an automated data acquisition system to provide test section velocities.

The data acquisition system is controlled by a Zenith 286 Advanced Technology Personal Computer. This computer, using a Hewlett Packard multiplexing Input/Output card, sets the lifting airfoil angle-of-attack and reads the pressure at each airfoil station for each requested α. A Scani-Valve transducer provides calibrated atmospheric, test section static, and airfoil pressures. Detailed descriptions of the data acquisition system can be found in Reference 6.

Selection of the test α range and target tunnel speed are controlled by software. However, tunnel speed is maintained solely by manual control. Whenever tunnel speed is detected by the software to exceed an offset of two feet per second from the desired speed the operator is advised to adjust back to the target speed.

A data file is output consisting of the desired α, static pressure, computed speed and dynamic pressure, and individual airfoil station pressures. The actual test α for each run is monitored by the operator and updated in the data file by hand.

APPENDIX B

Two computer programs were written for this thesis by the author. Each program was written in QuickBASIC and used for data manipulation. The programs were called CPDATA.EXE and CLDATA.EXE.

The CPDATA.EXE program accepted as input the data file provided by the automated data acquisition system. CPDATA.EXE then ordered the lifting airfoil's individual coefficients of pressure into upper and lower surface data. This ordered data was then output to another file along with Reynolds Number and the test angles-of-attack. The new data file could then be split into individual files for each angle-of-attack for input into graphics software.

Lift curves were computed using the CLDATA.EXE program. The raw test data file containing the test conditions and pressure distributions for an angle-of-attack sweep was input into the CLDATA program. The lift coefficient was calculated by trapezoidal integration of the pressure coefficients.

APPENDIX C

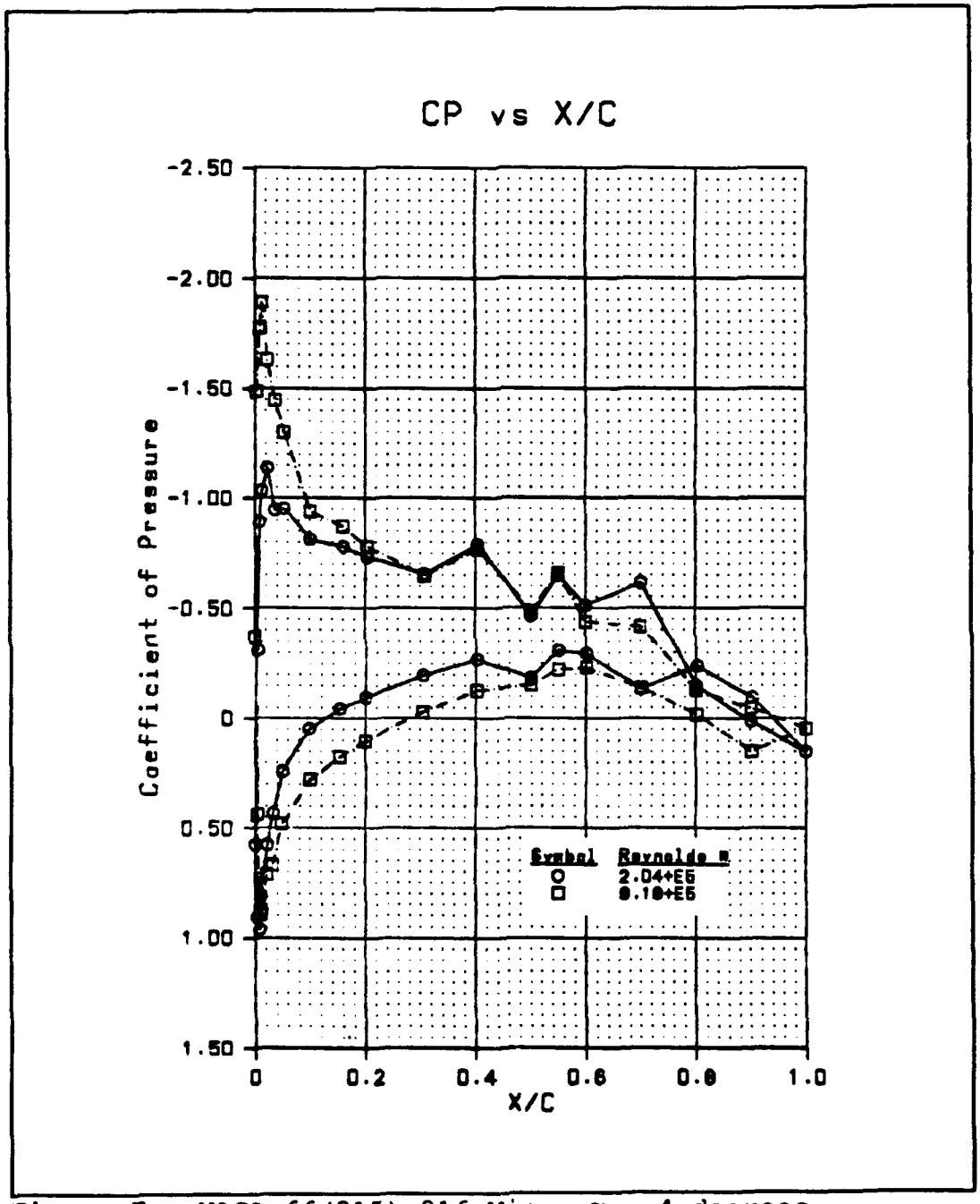

Figure 7. NACA 66(215)-216 Wing, α = 4 degrees

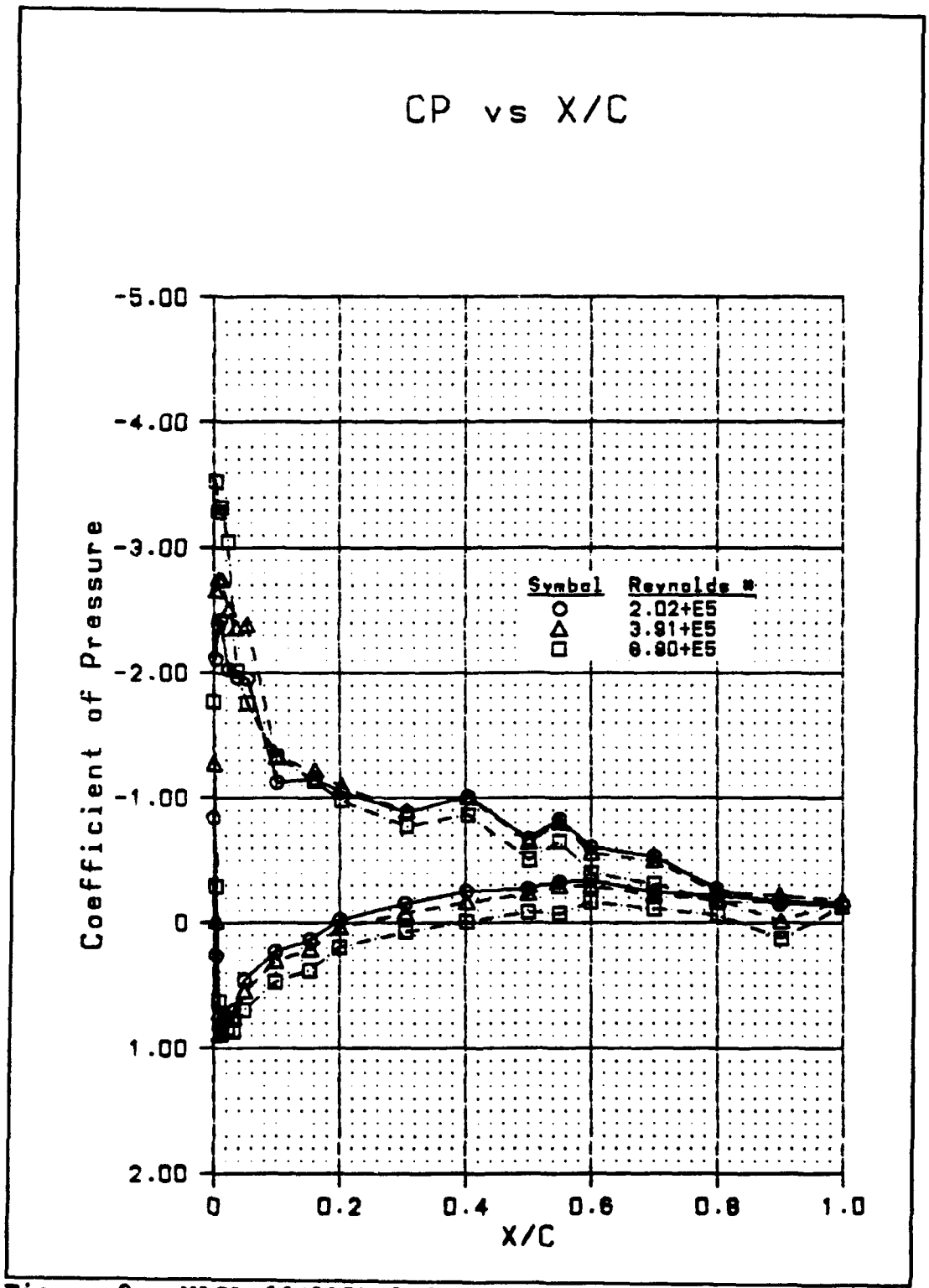

Figure 8. NACA 66(215)-216 Wing, α = 8 degrees

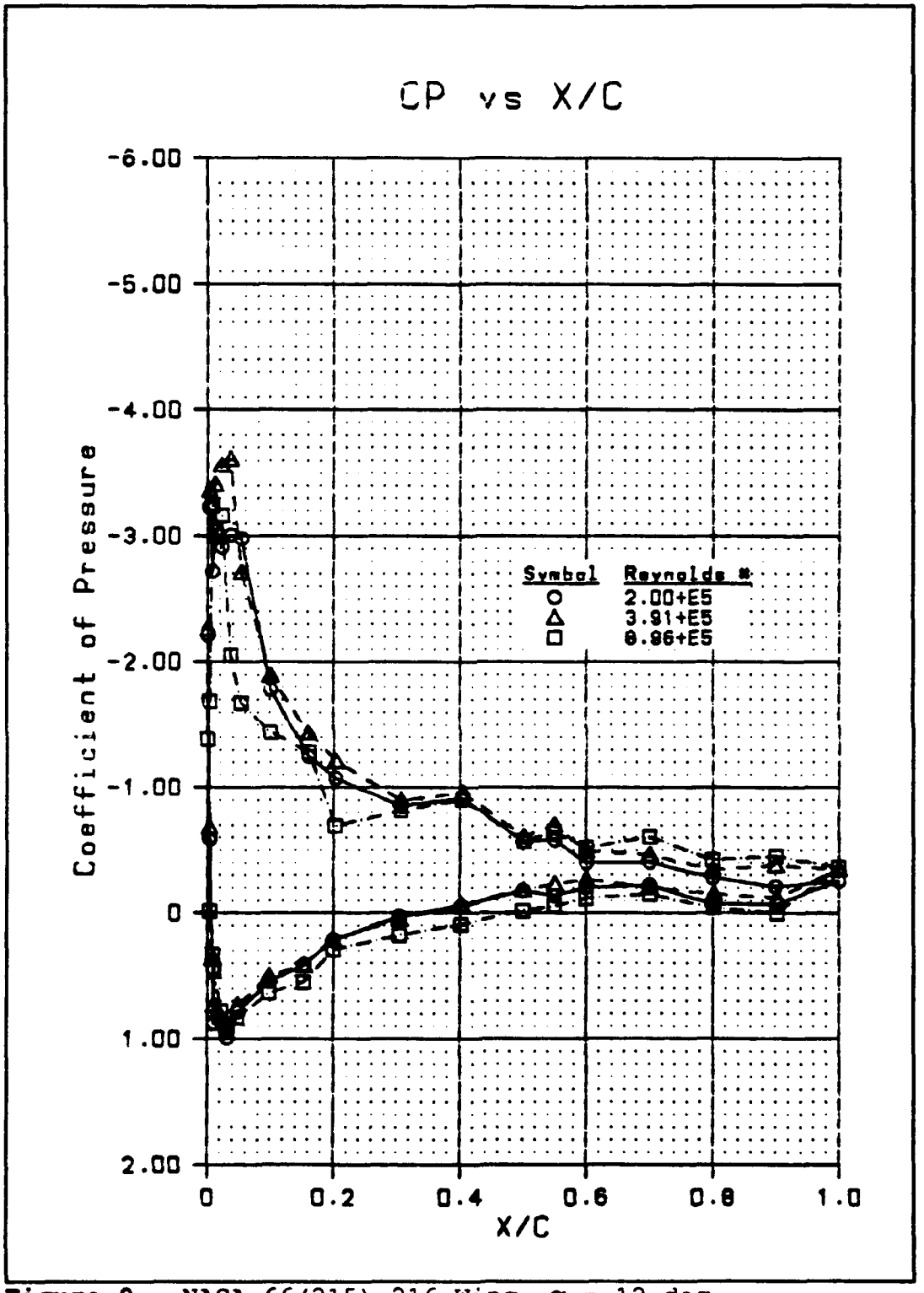

Figure 9. NACA 66(215)-216 Wing, α = 12 deg

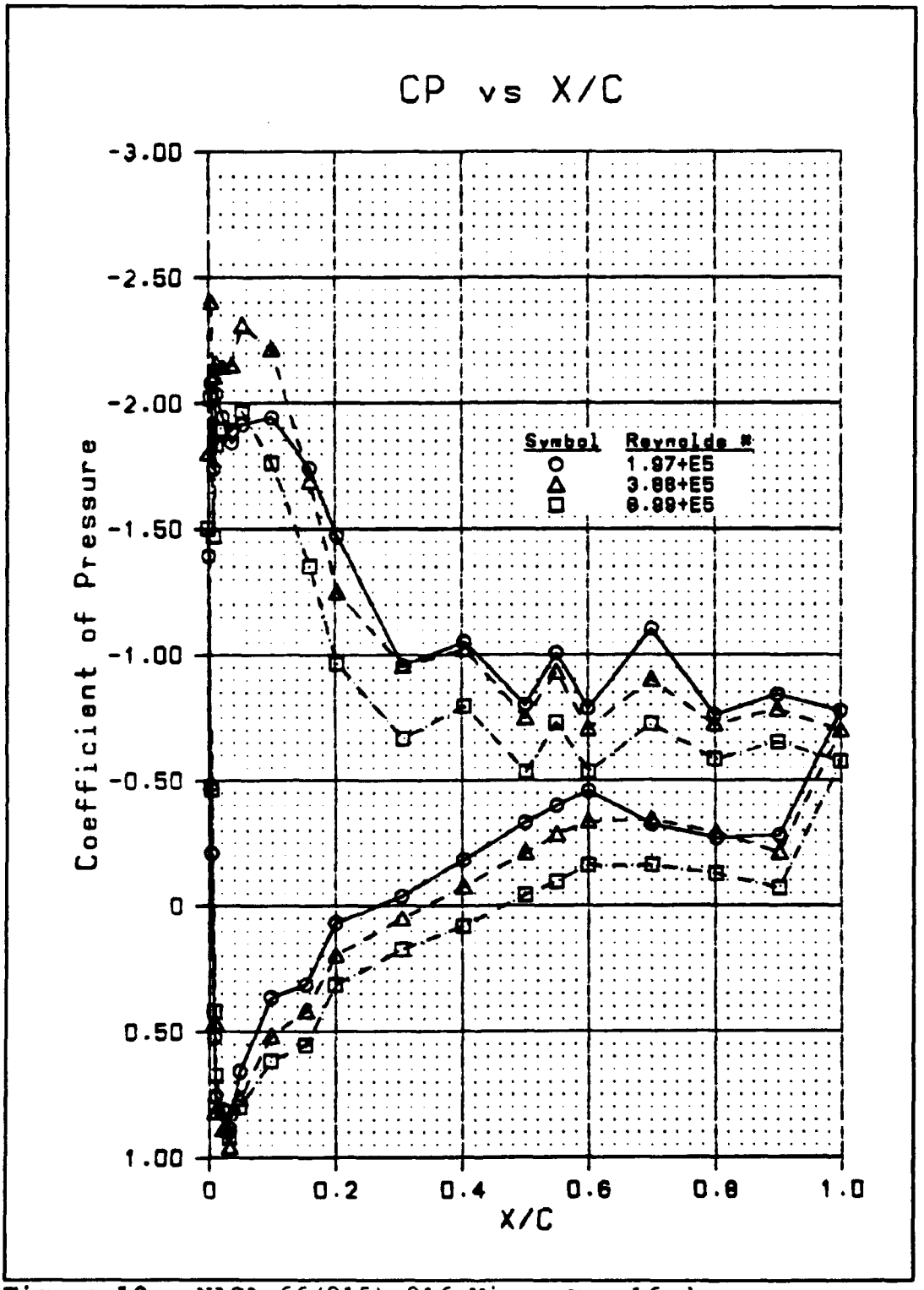

Figure 10. NACA 66(215)-216 Wing, α = 16 deg

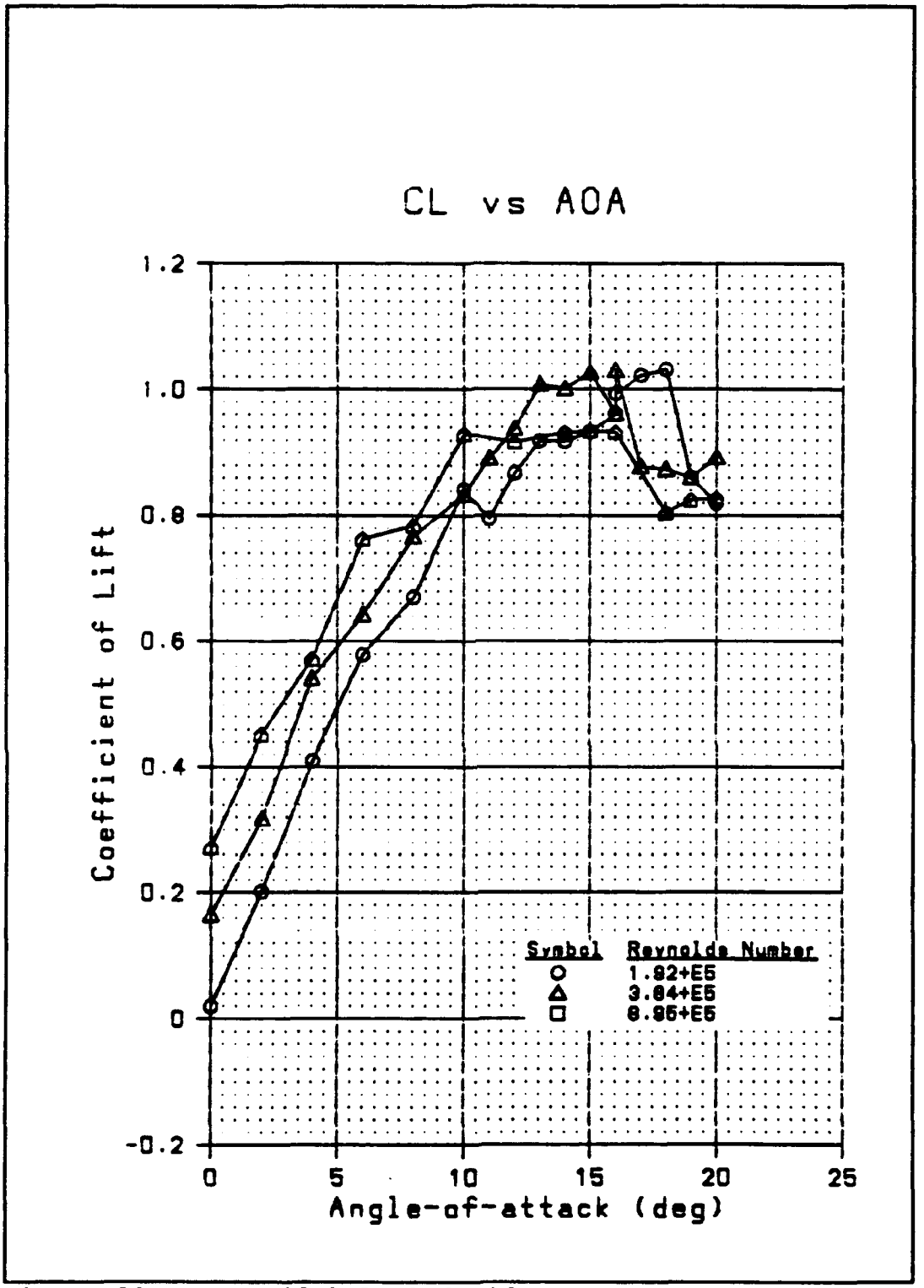

Figure 11. NACA 66(215)-216 Lift Curves

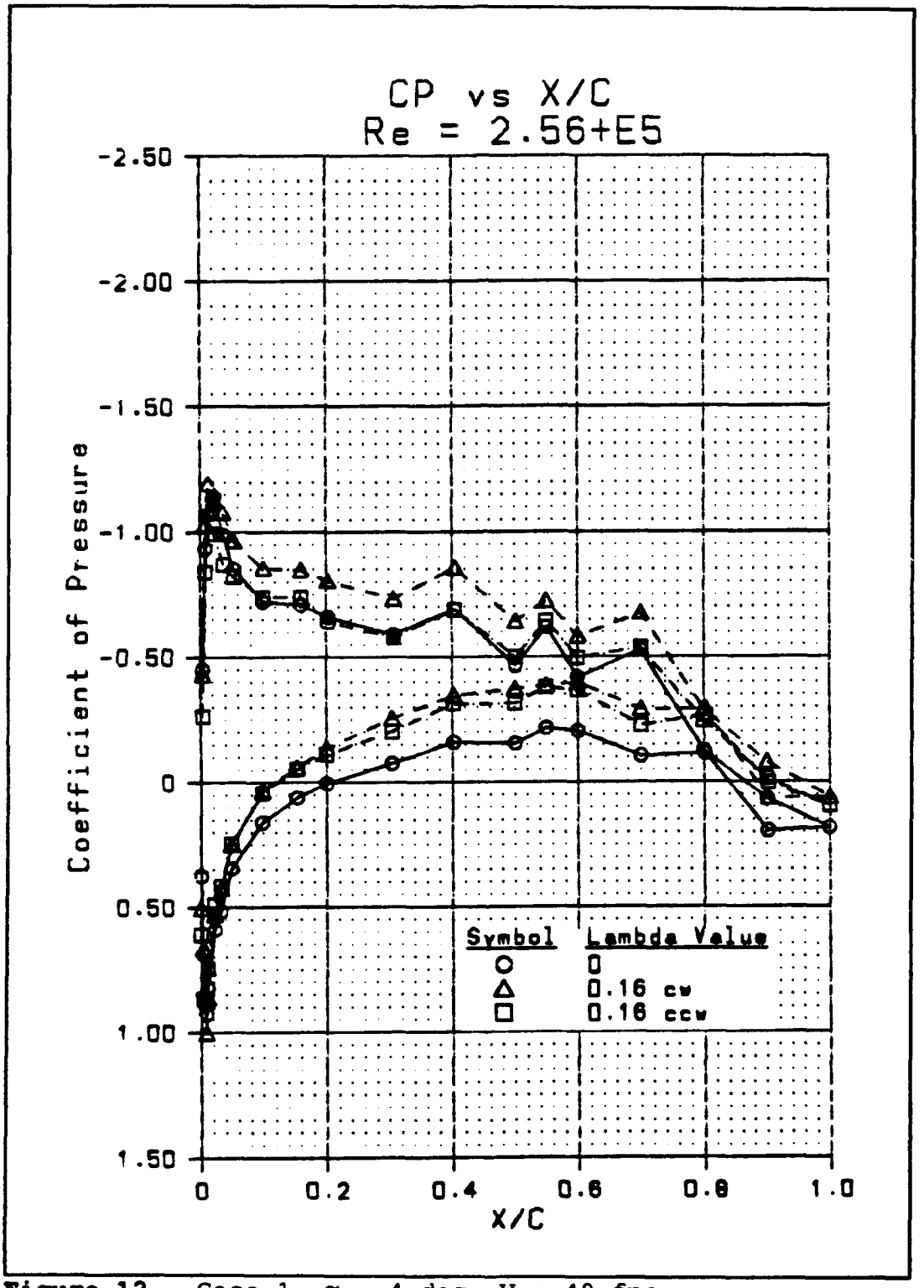

Figure 12. Case 1, α = 4 deg, V = 40 fps

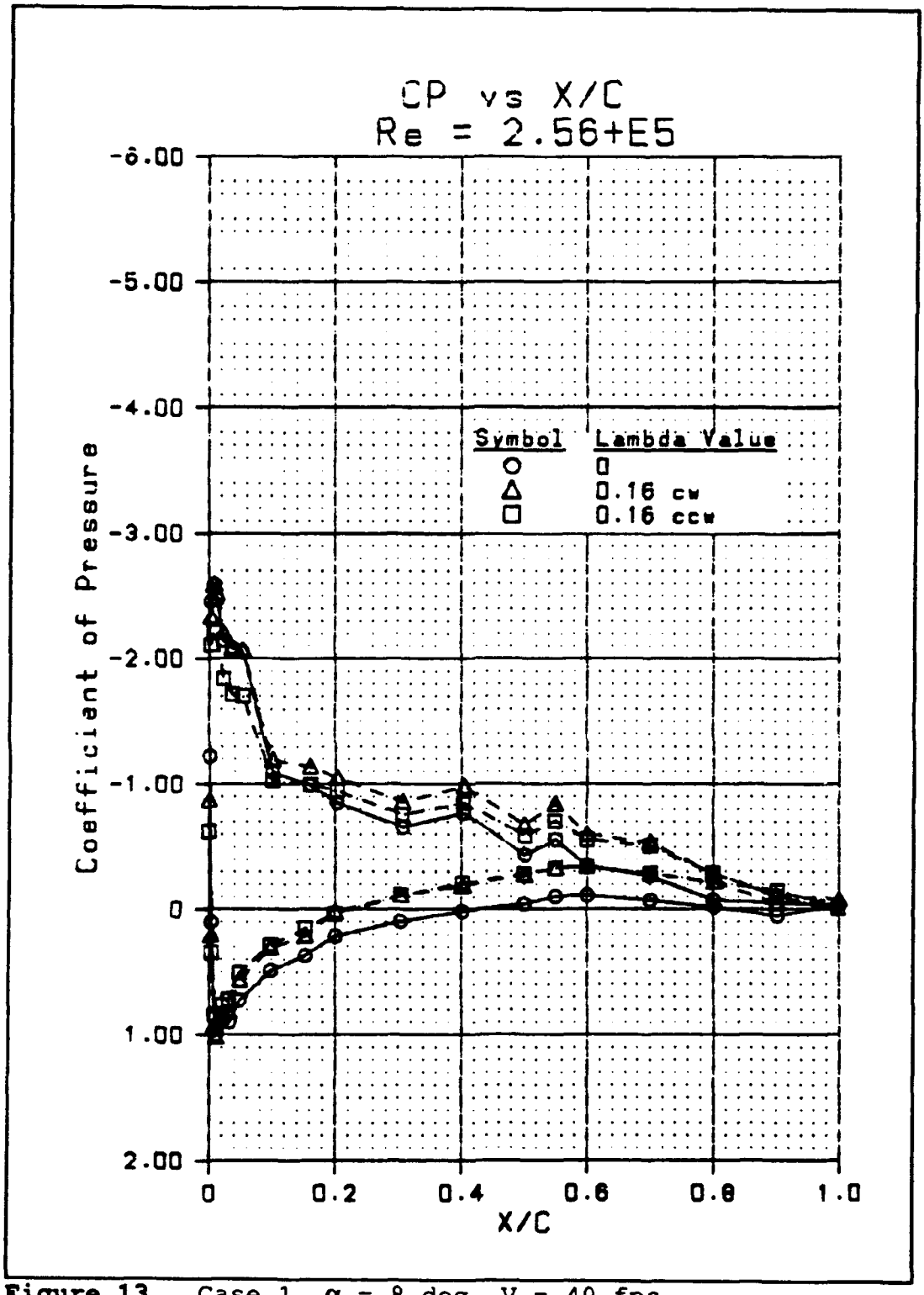

Figure 13. Case 1, α = 8 deg, V = 40 fps

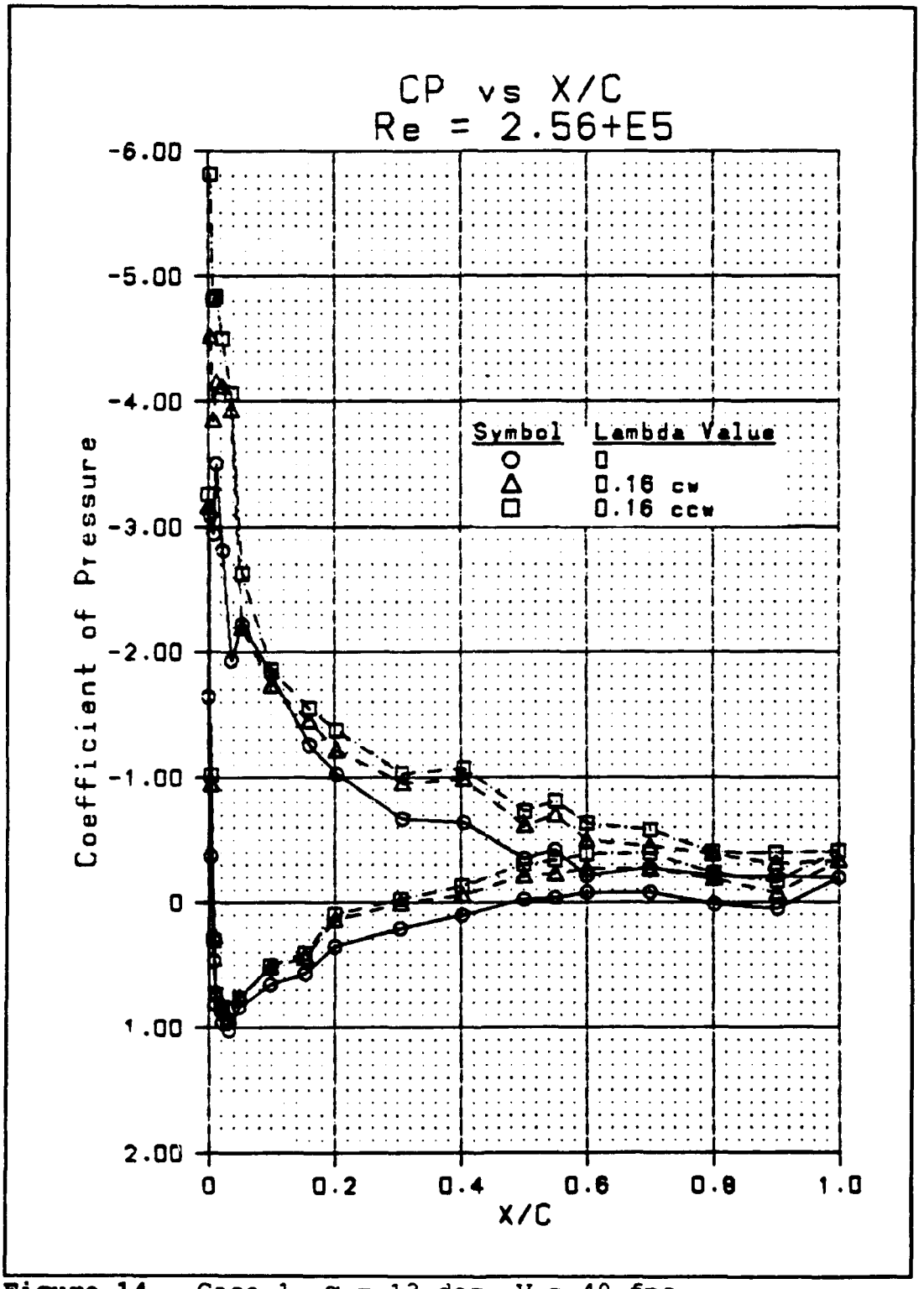

Figure 14. Case 1, α = 13 deg, V = 40 fps

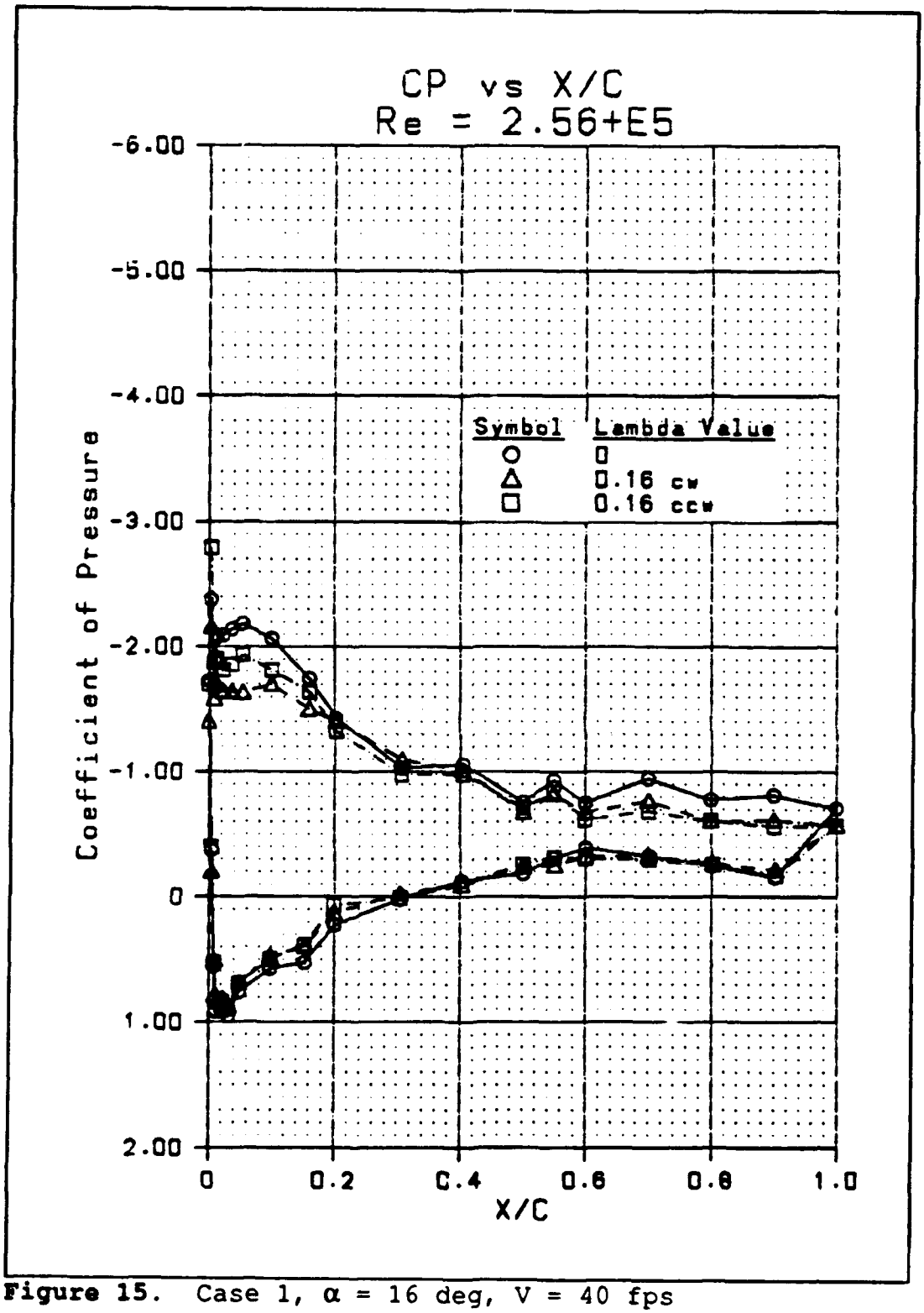

Figure 15. Case 1, α = 16 deg, V = 40 fps

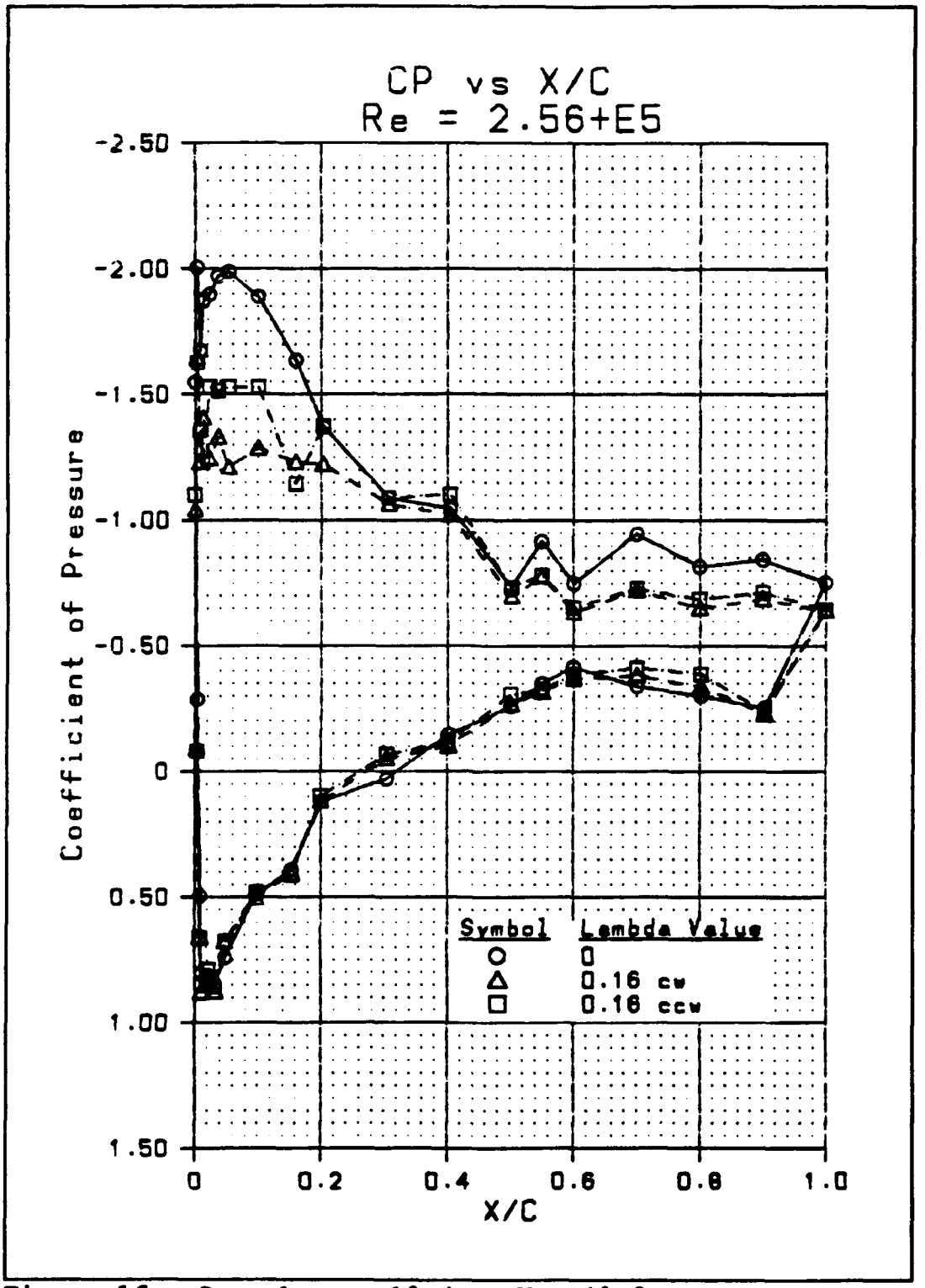

Figure 16. Case 1, α = 18 deg, V = 40 fps

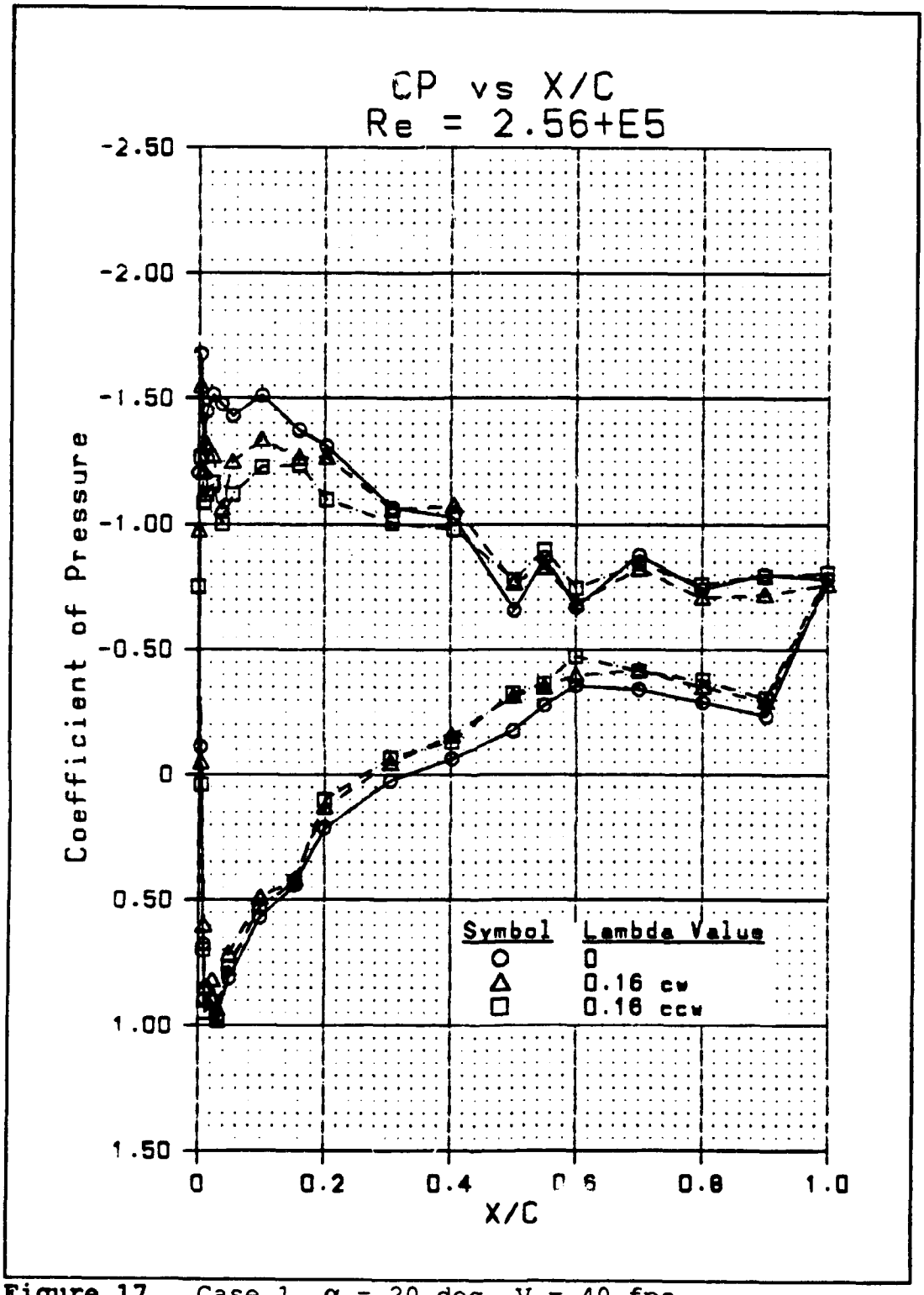

Figure 17. Case 1, α = 20 deg, V = 40 fps

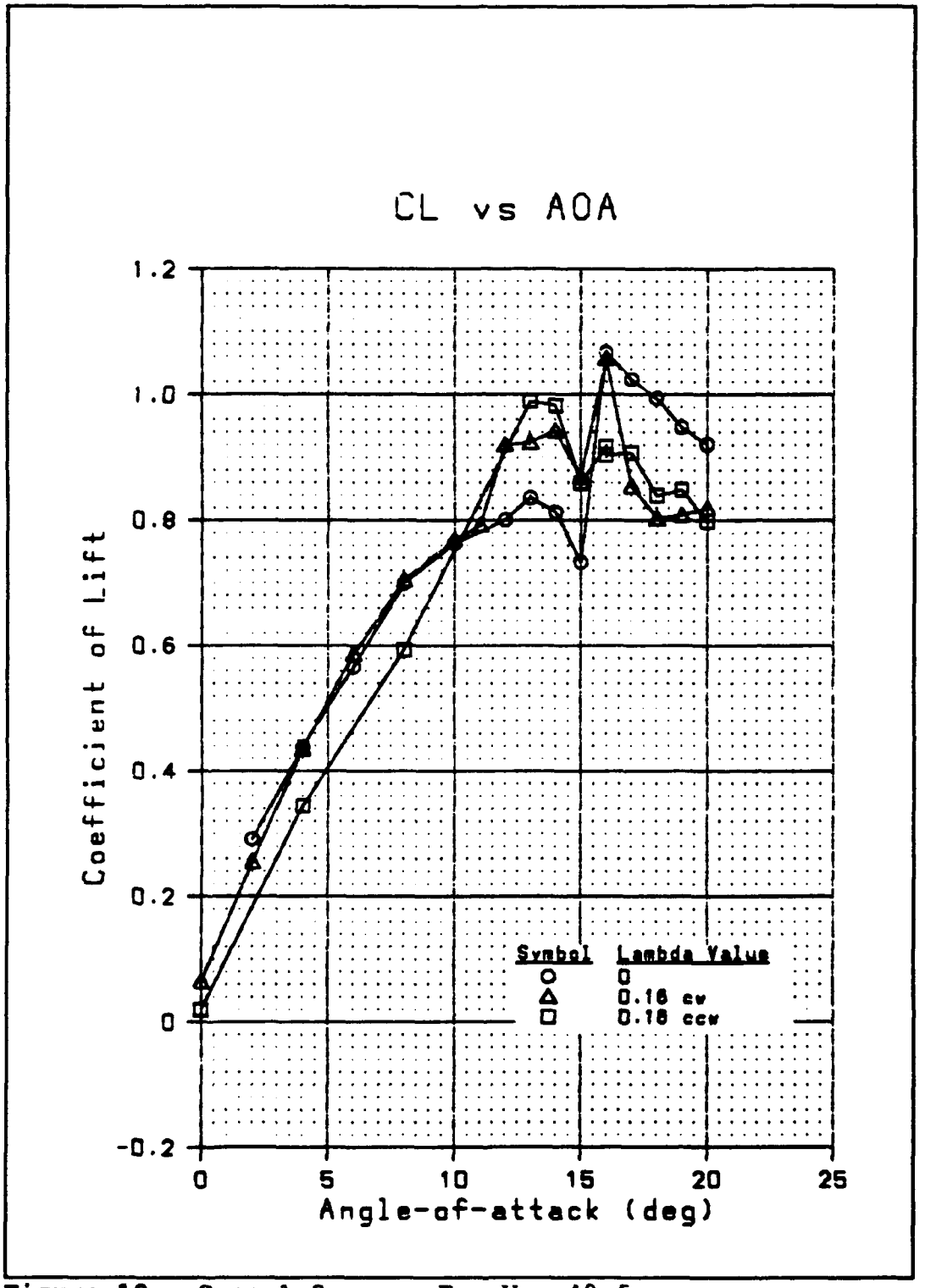

Figure 18. Case 1 Summary For V = 40 fps

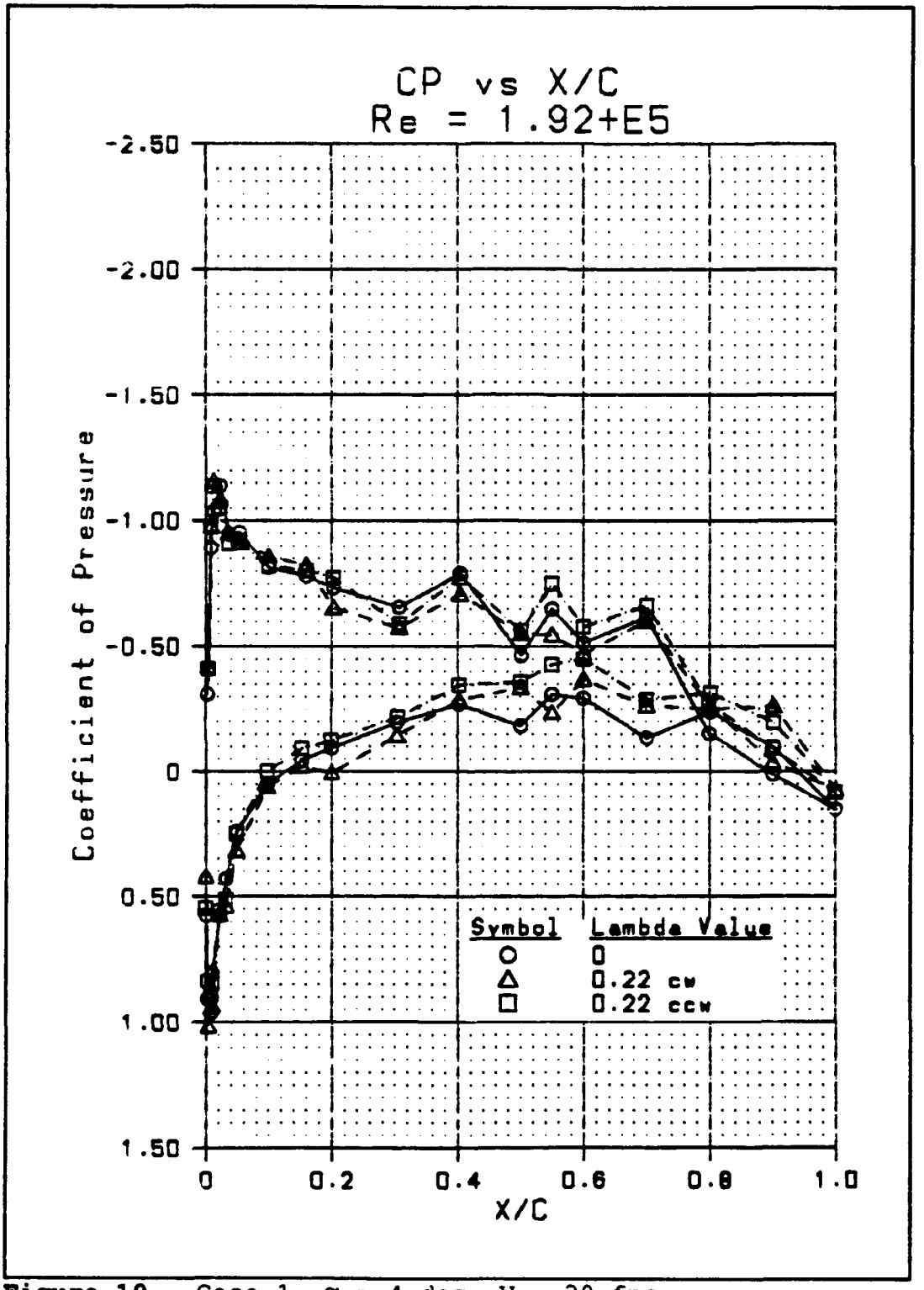

Figure 19. Case 1, α = 4 deg, V = 30 fps

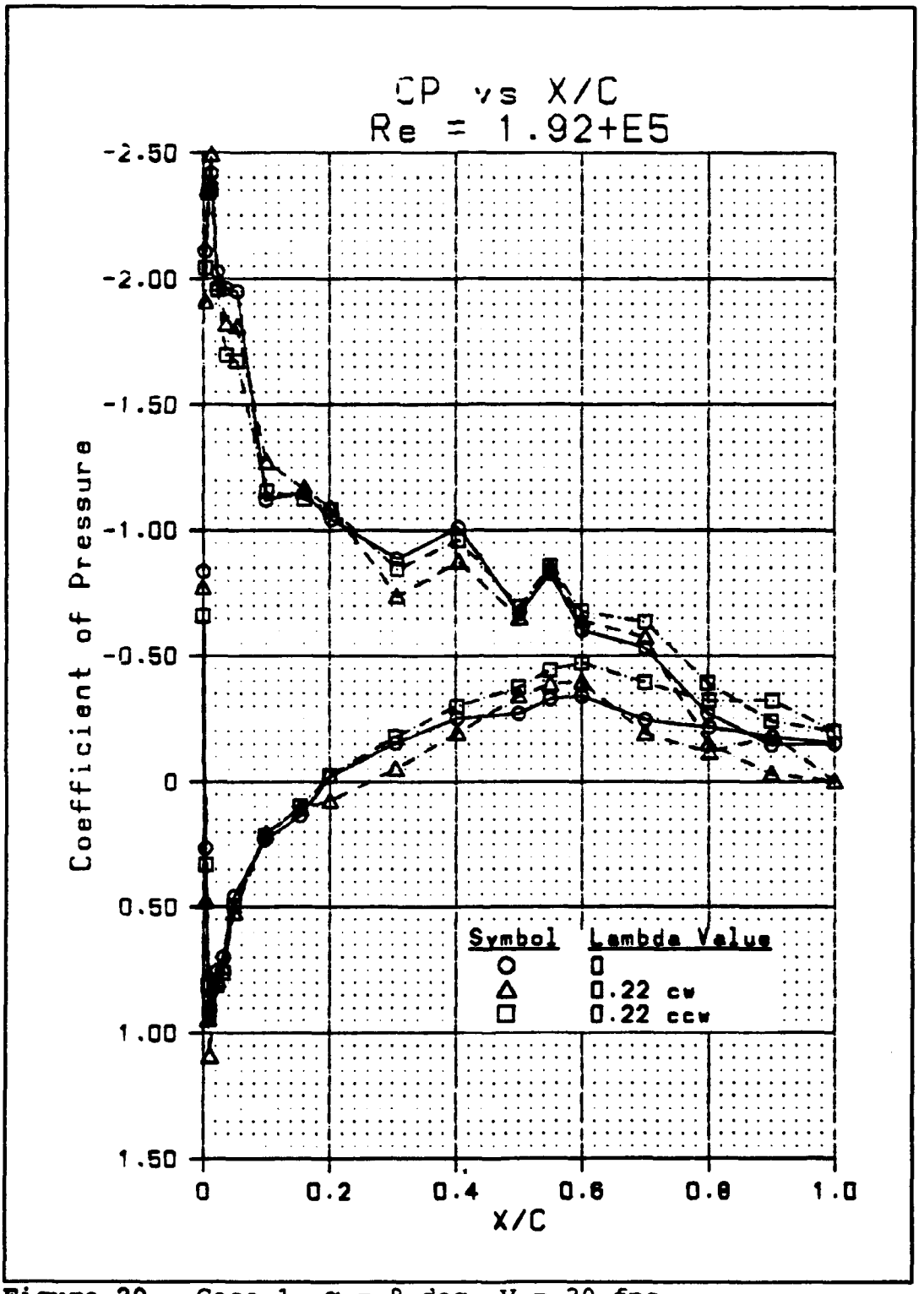

Figure 20. Case 1, α = 8 deg, V = 30 fps

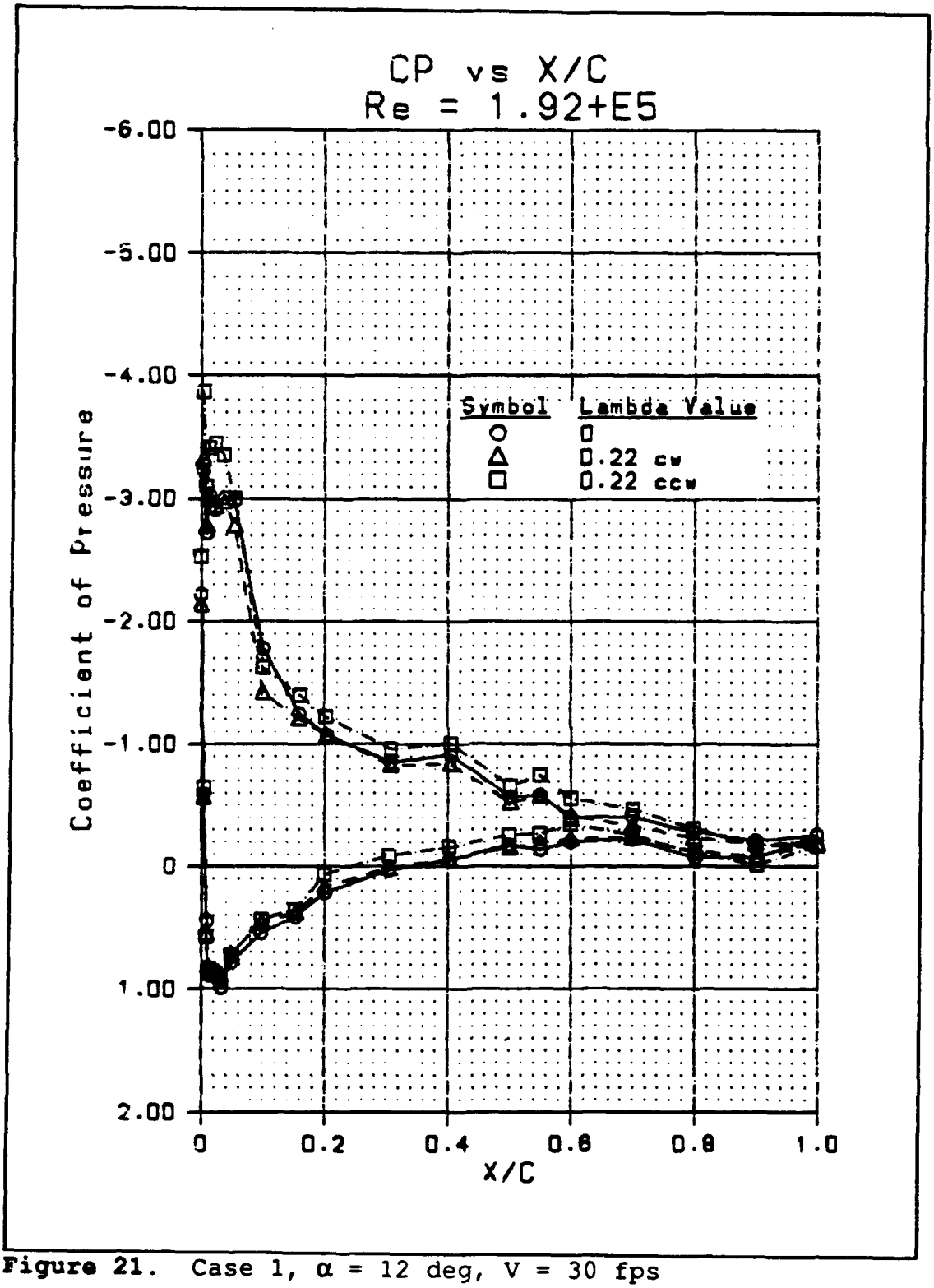

Figure 21. Case 1, α = 12 deg, V = 30 fps

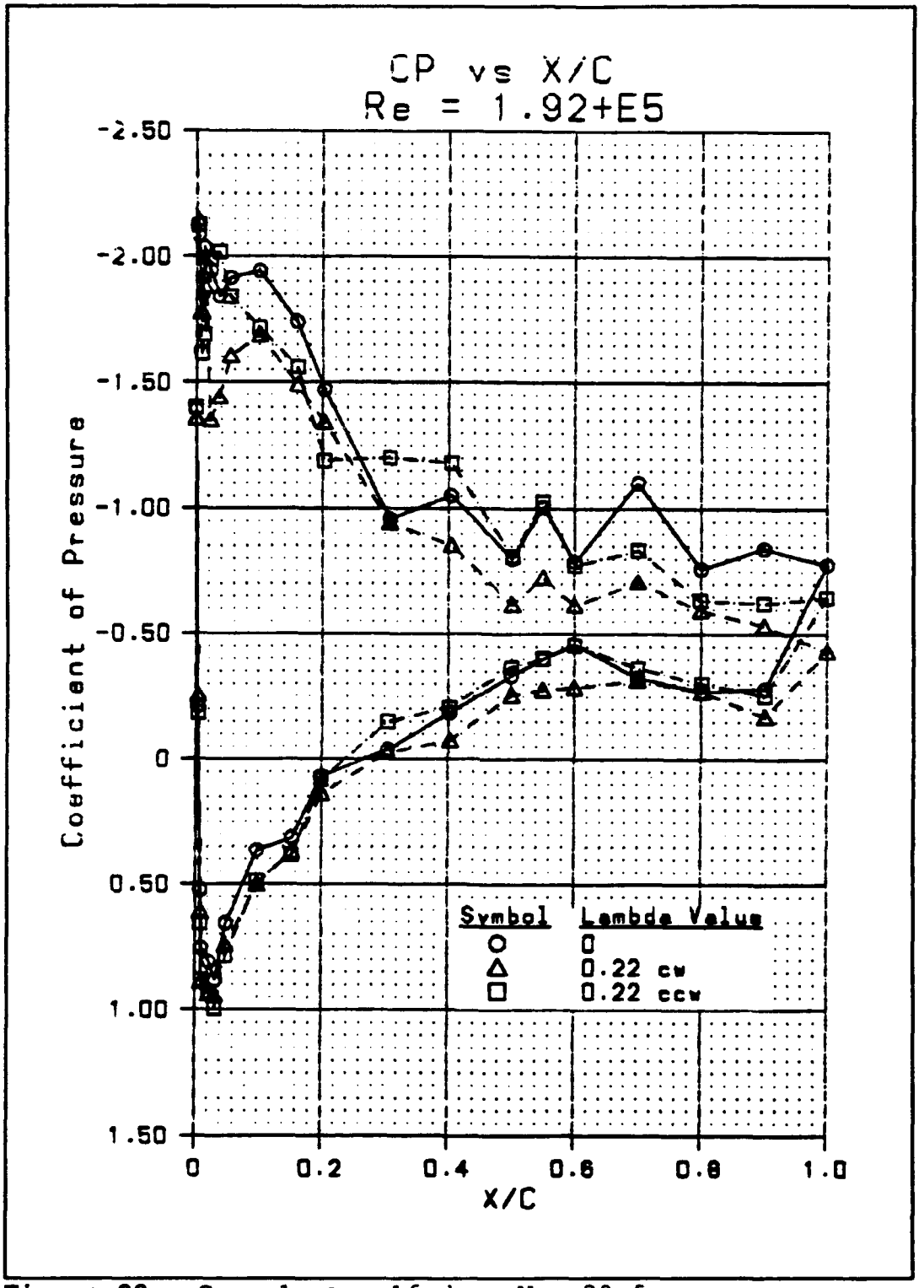

Figure 22. Case 1, α = 16 deg, V = 30 fps

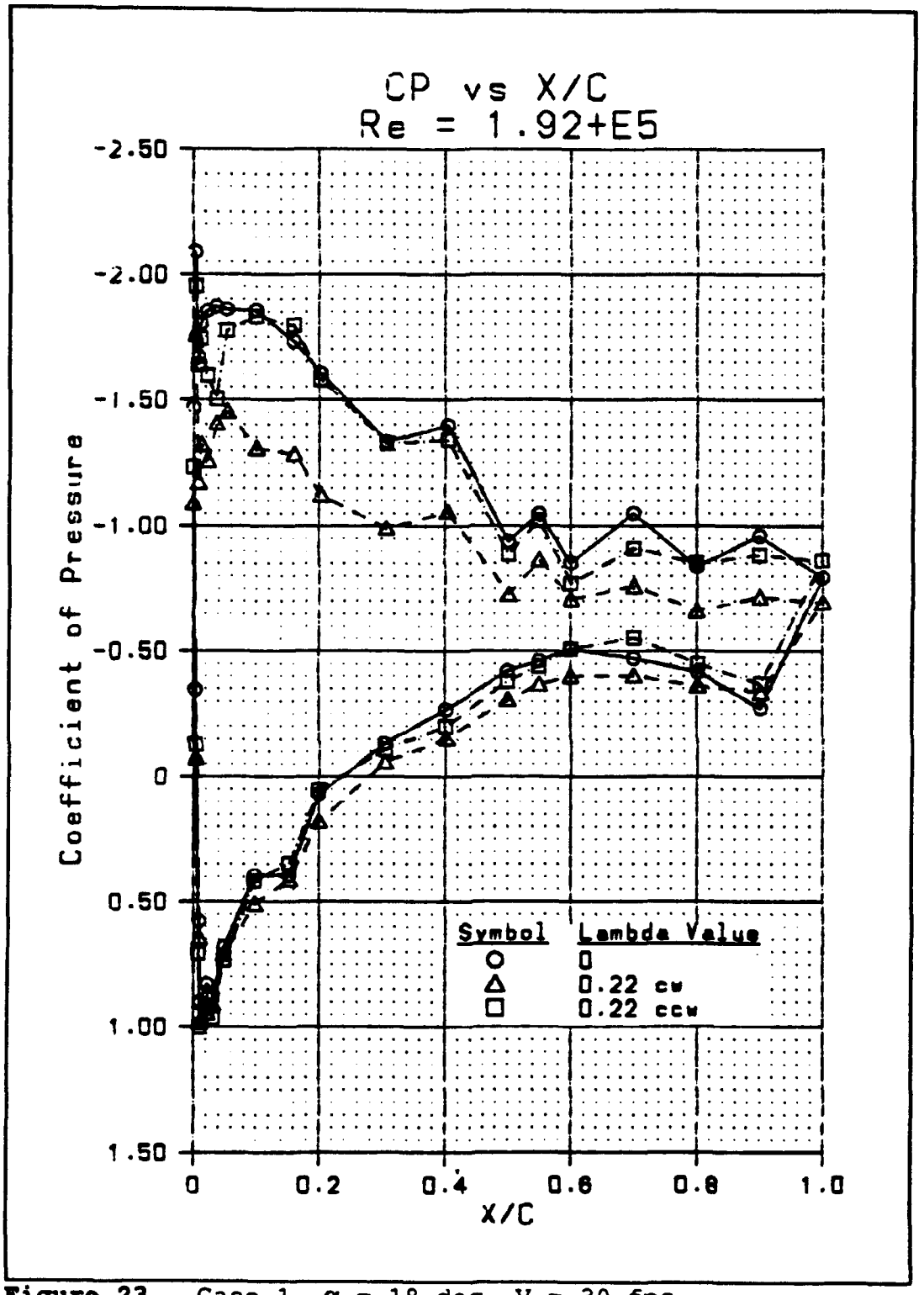

Figure 23. Case 1, α = 18 deg, V = 30 fps

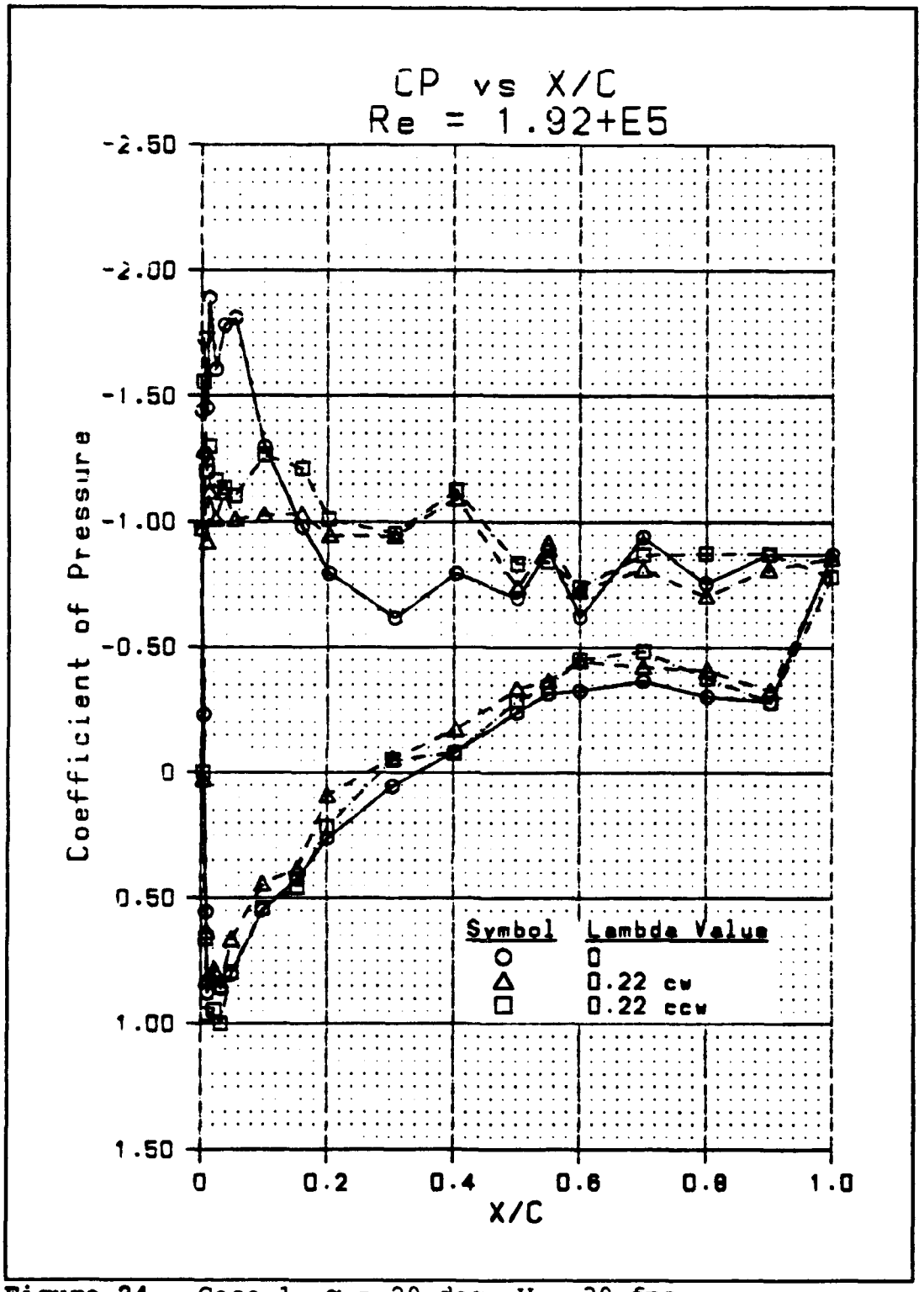

Figure 24. Case 1, α = 20 deg, V = 30 fps

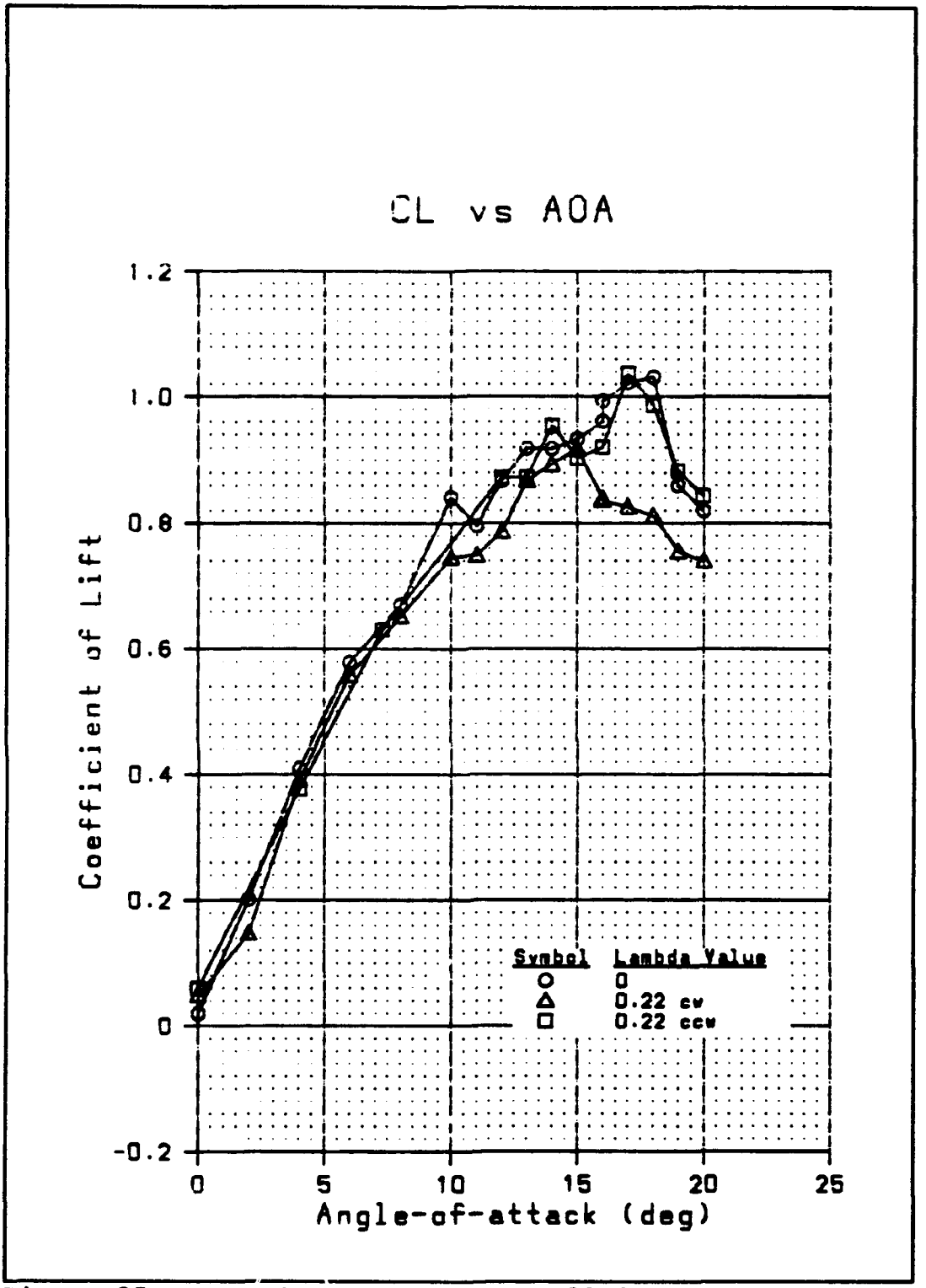

Figure 25. Case 1 Summary For V = 30 fps

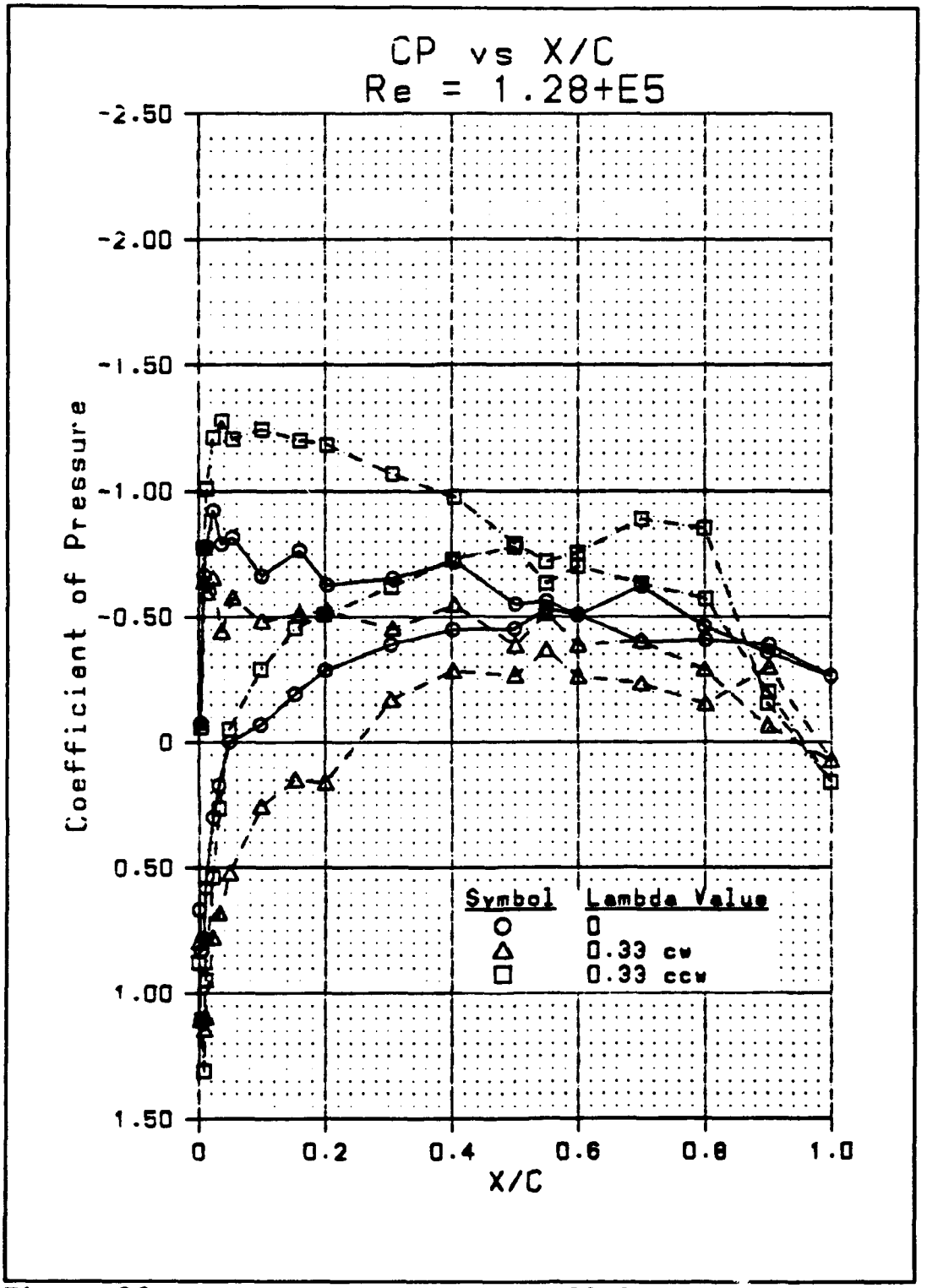

Figure 26. Case 1, α = 4 deg, V = 20 fps

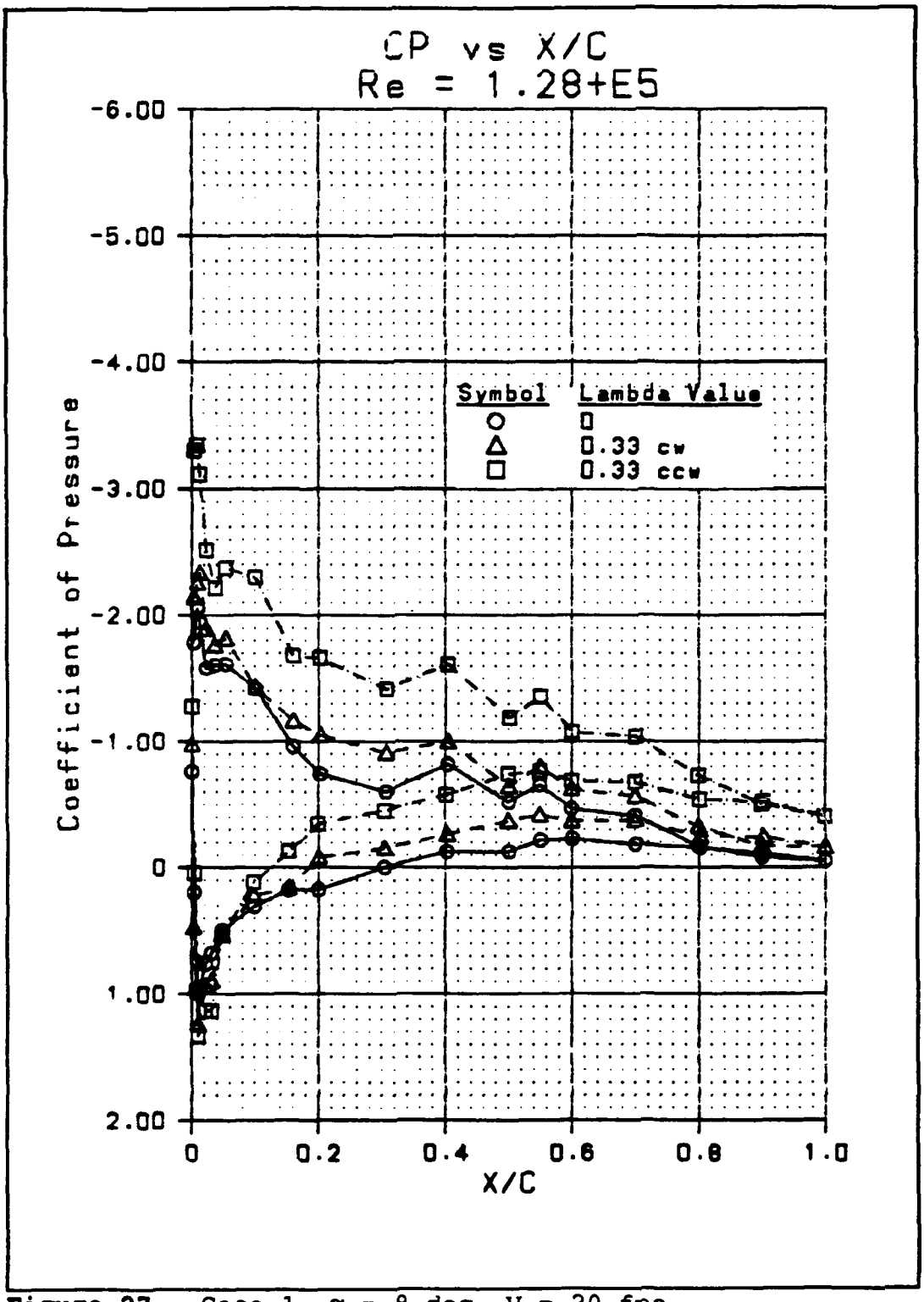

Figure 27. Case 1, α = 8 deg, V = 20 fps

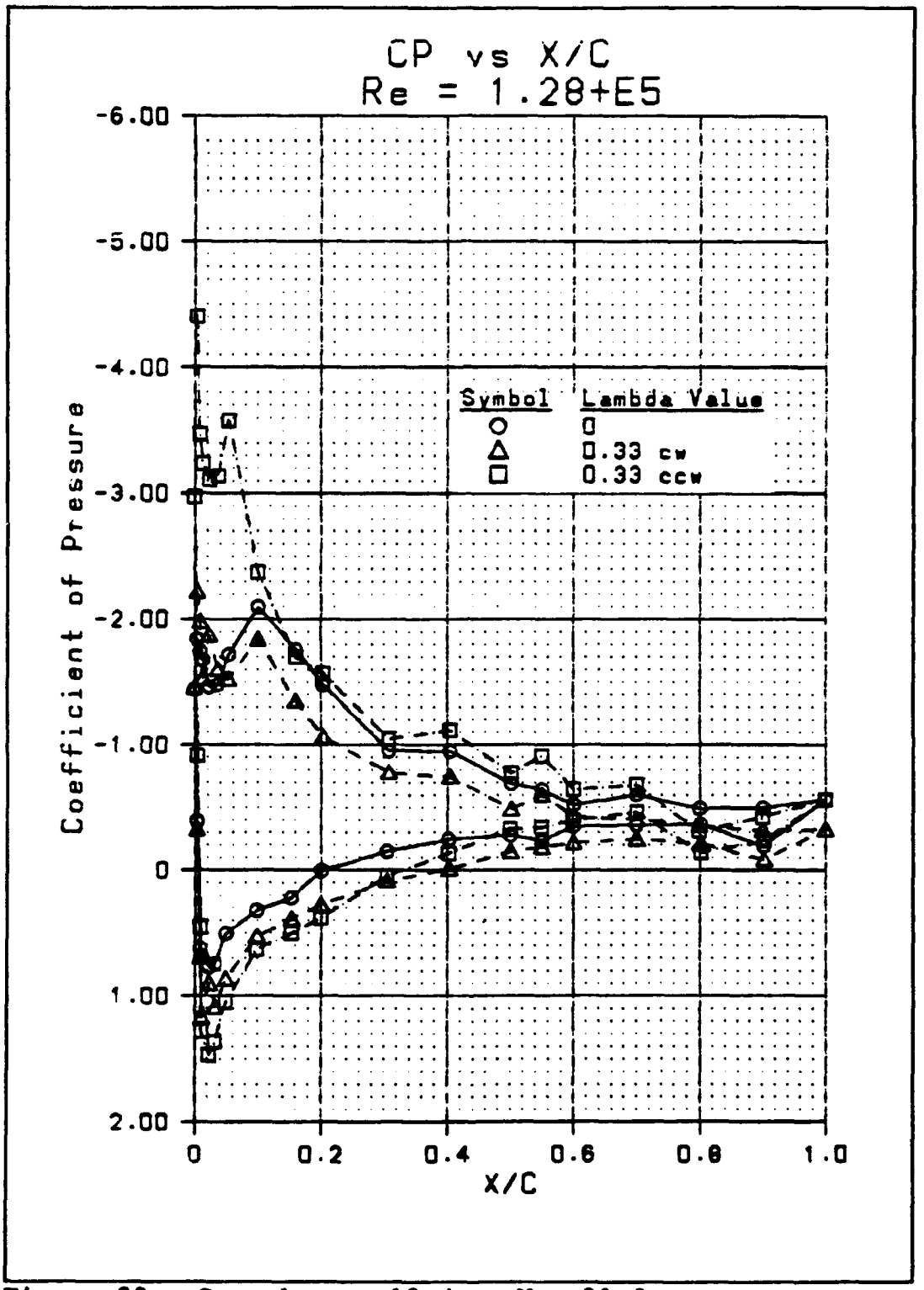

Figure 28. Case 1, α = 13 deg, V = 20 fps

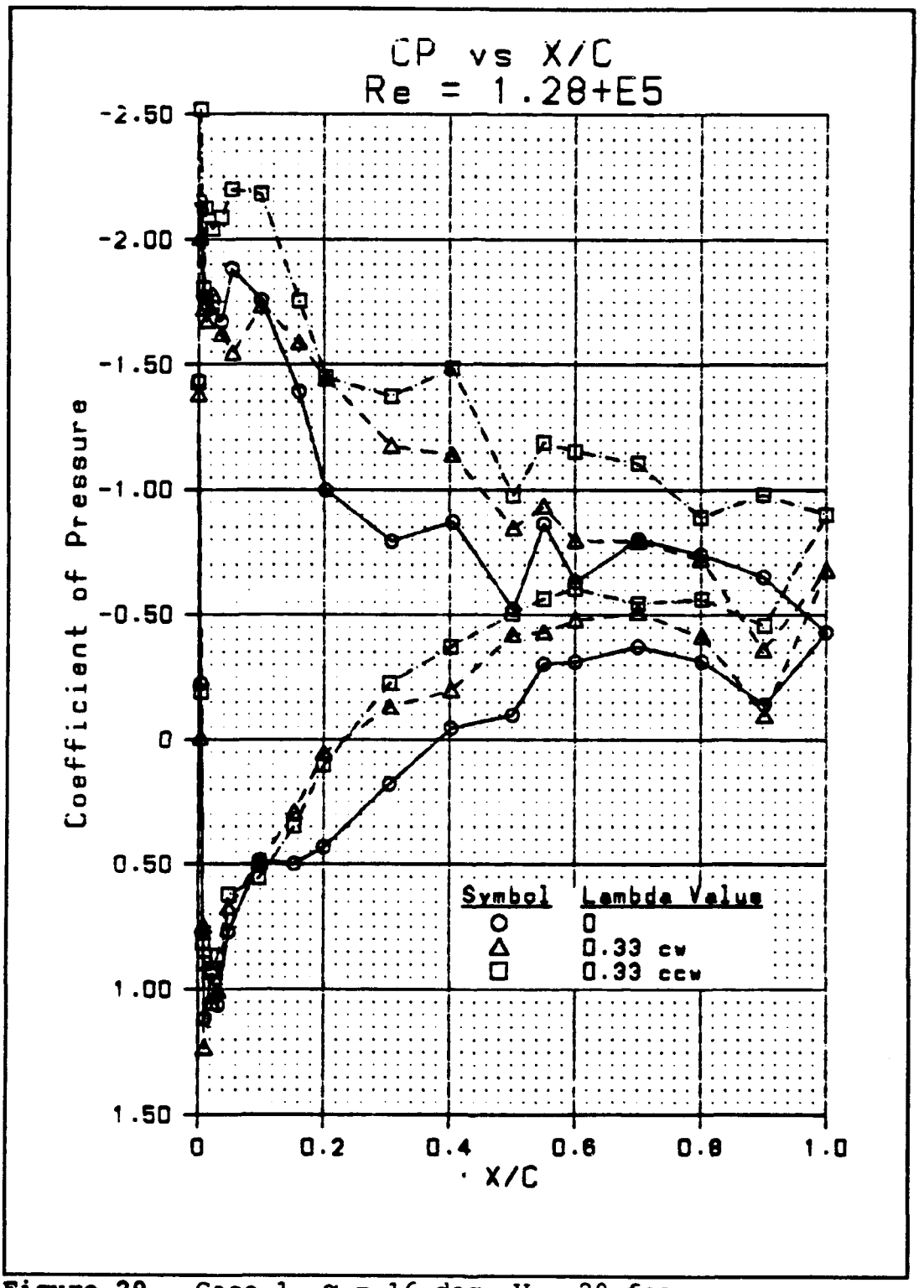

Figure 29. Case 1, α = 16 deg, V = 20 fps

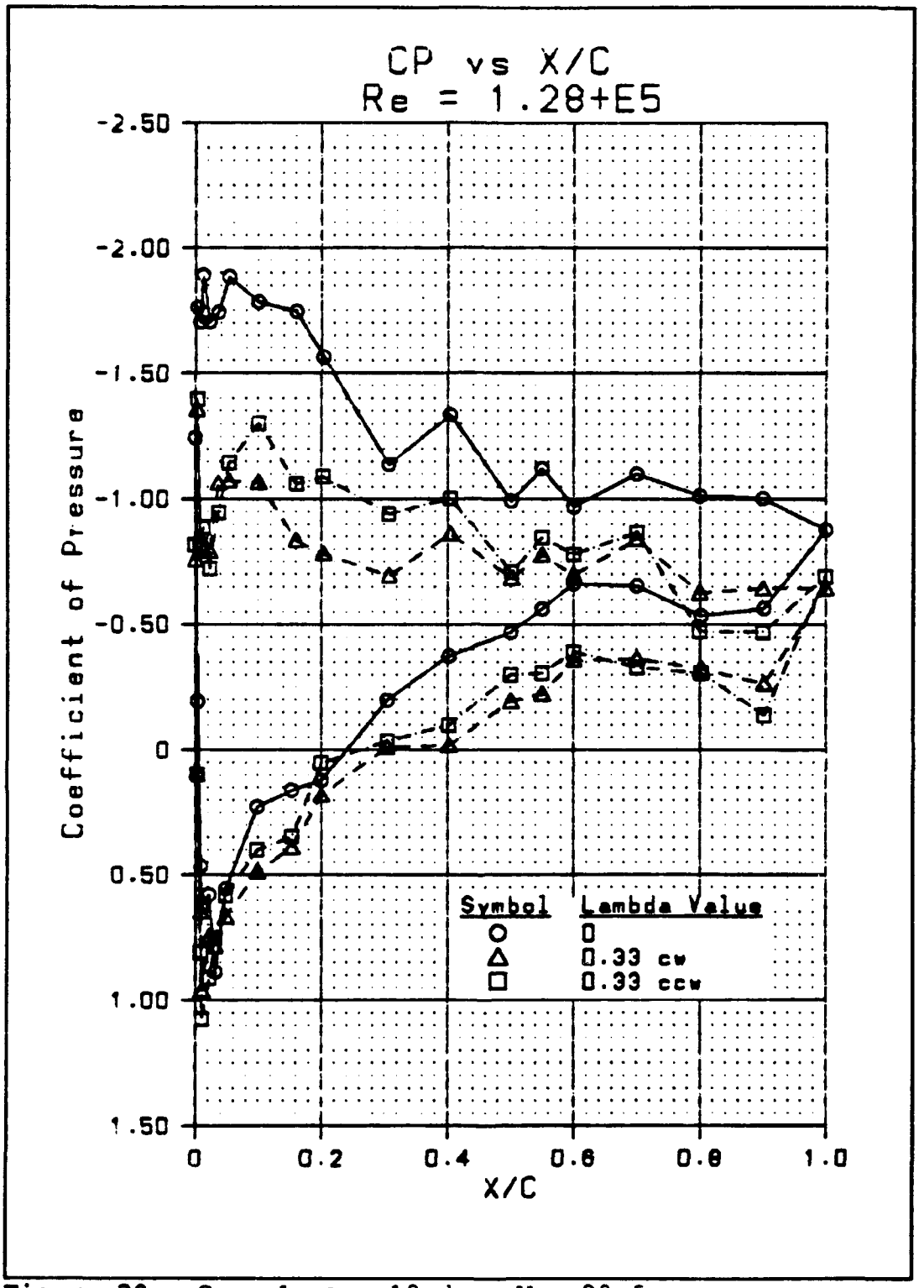

Figure 30. Case 1, α = 18 deg, V = 20 fps

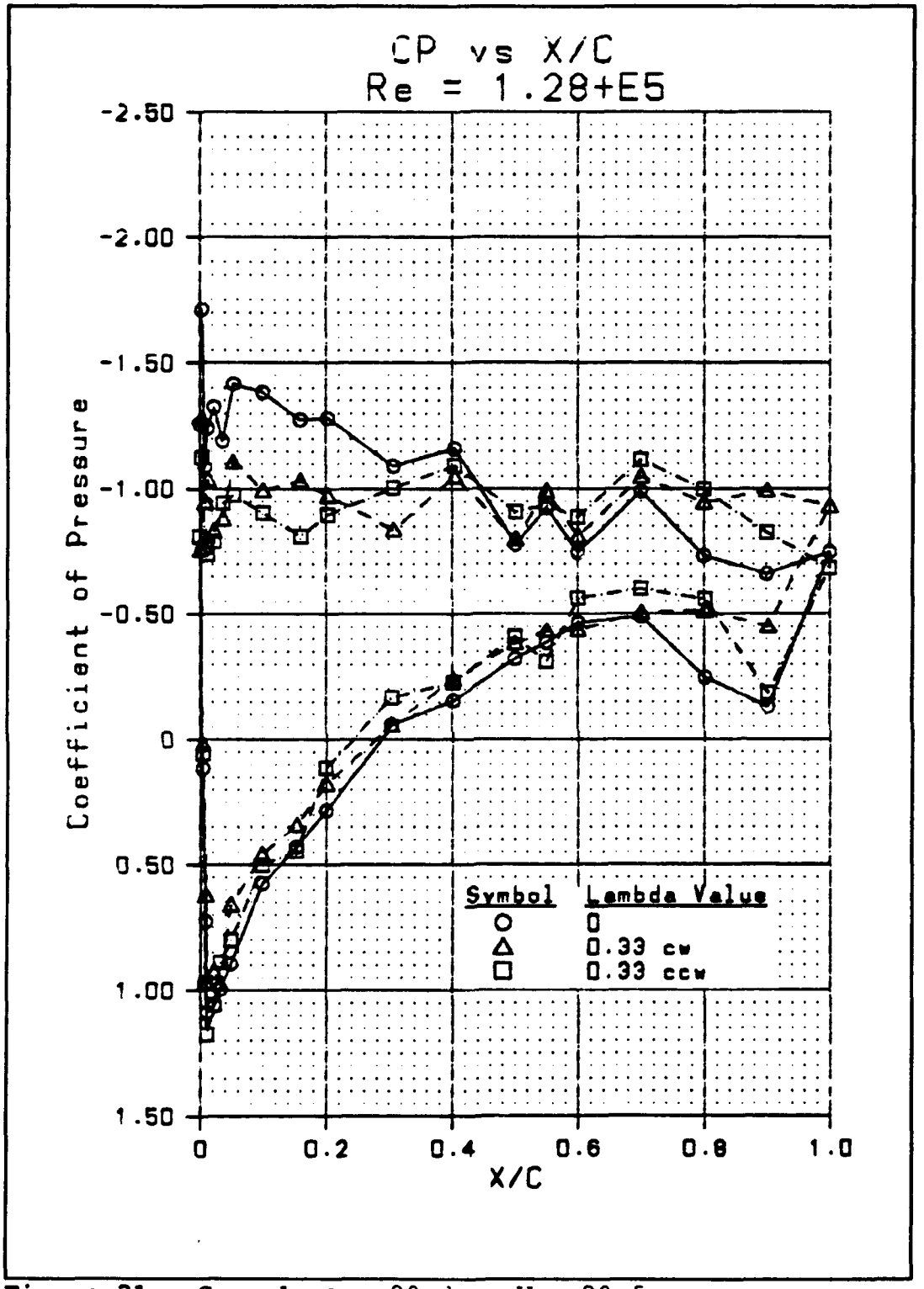

Figure 31. Case 1, α = 20 deg, V = 20 fps

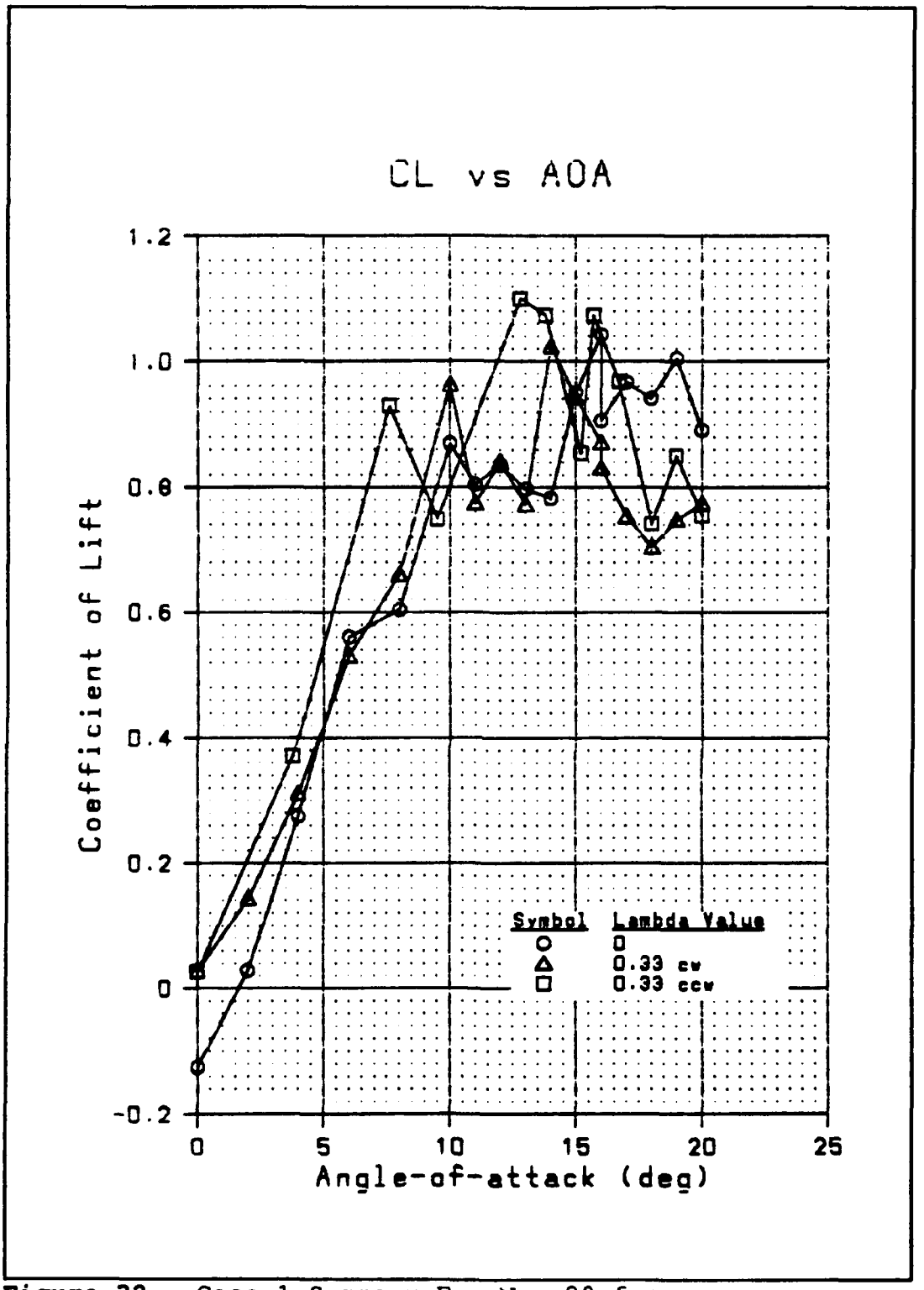

Figure 32. Case 1 Summary For V = 20 fps

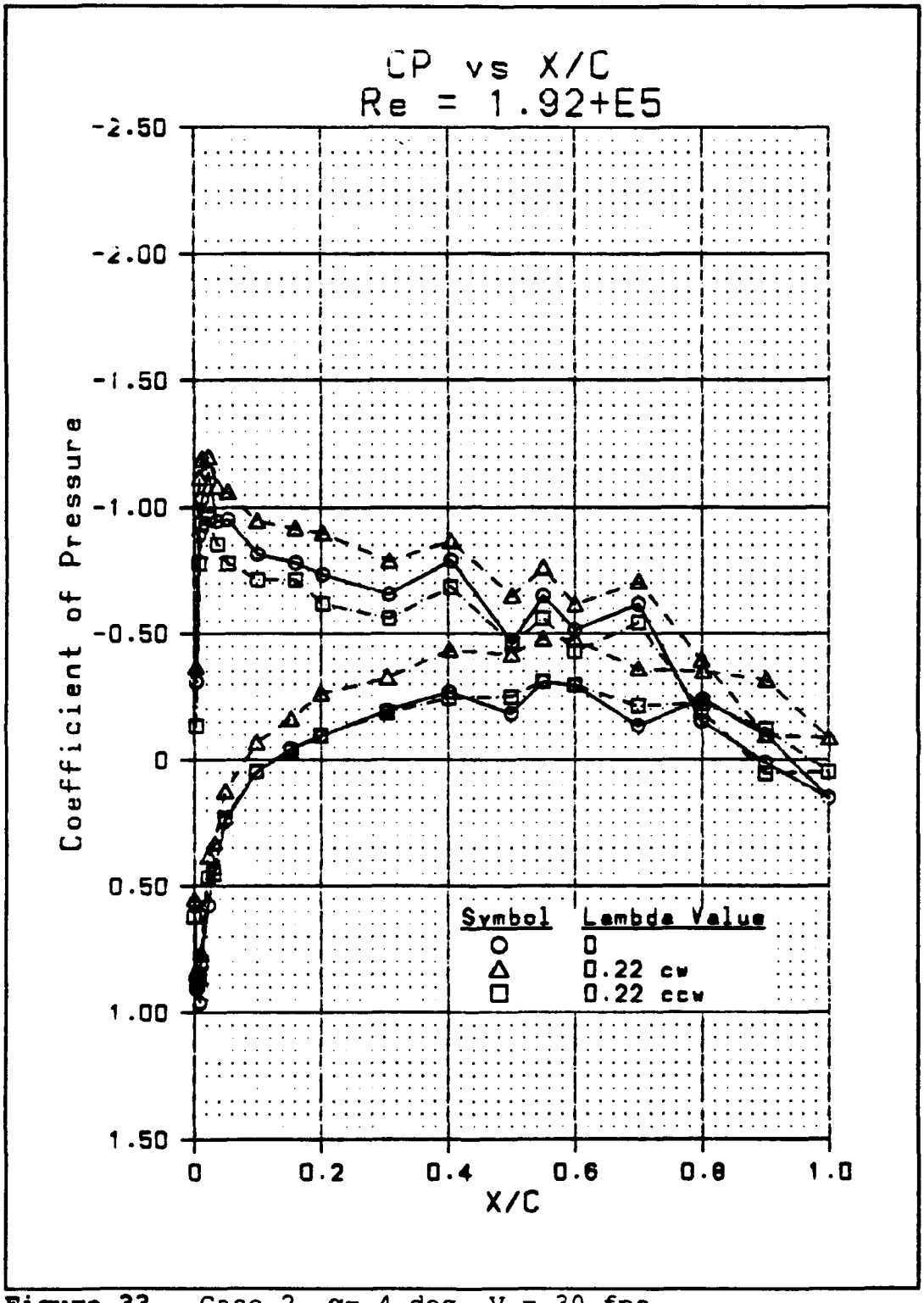

Figure 33. Case 2, α= 4 deg, V = 30 fps

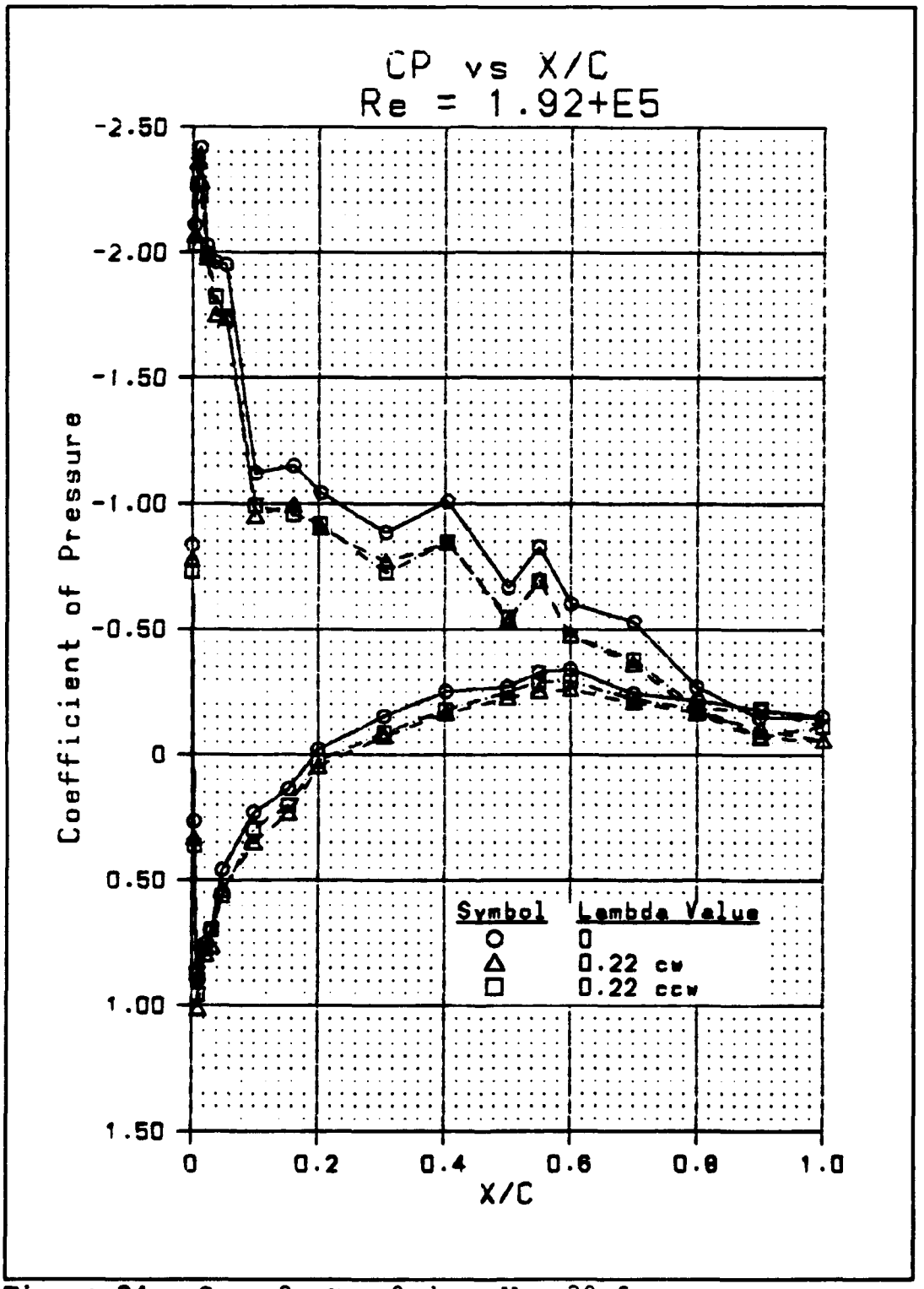

Figure 34. Case 2, α = 8 deg, V = 30 fps

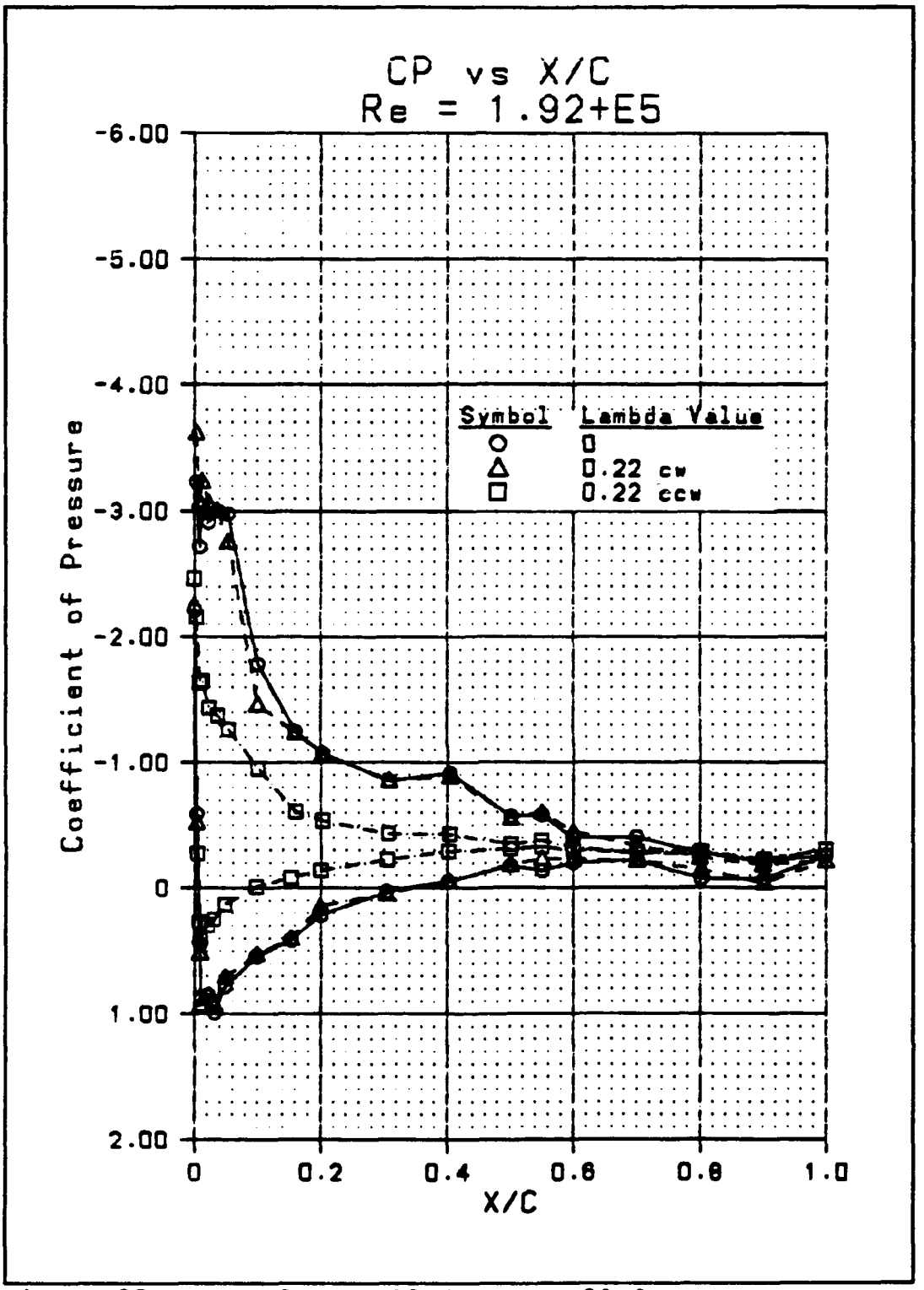

Figure 35. Case 2, α = 12 deg, V = 30 fps

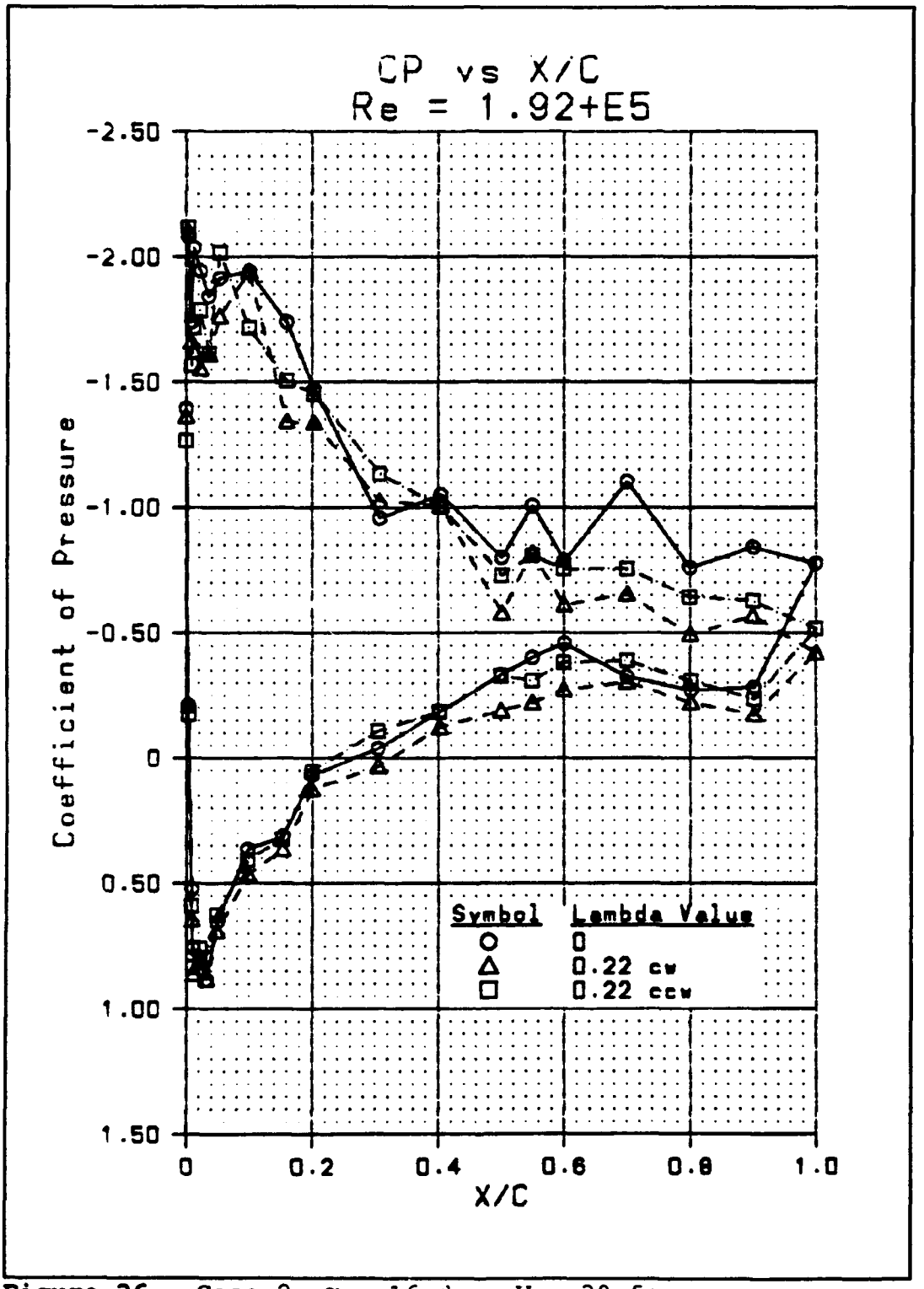

Figure 36. Case 2, α = 16 deg, V = 30 fps

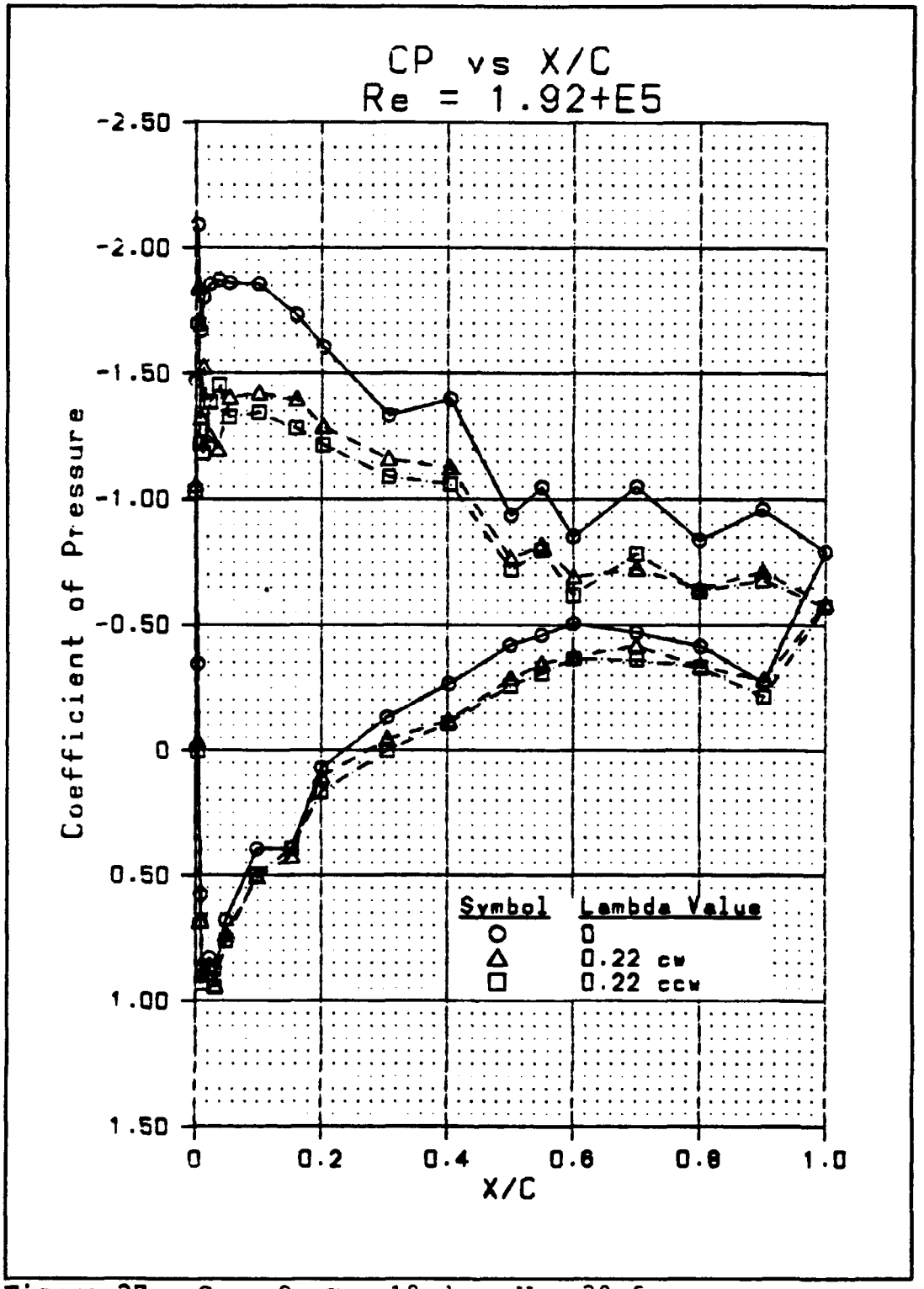

Figure 37. Case 2, α = 18 deg, V = 30 fps

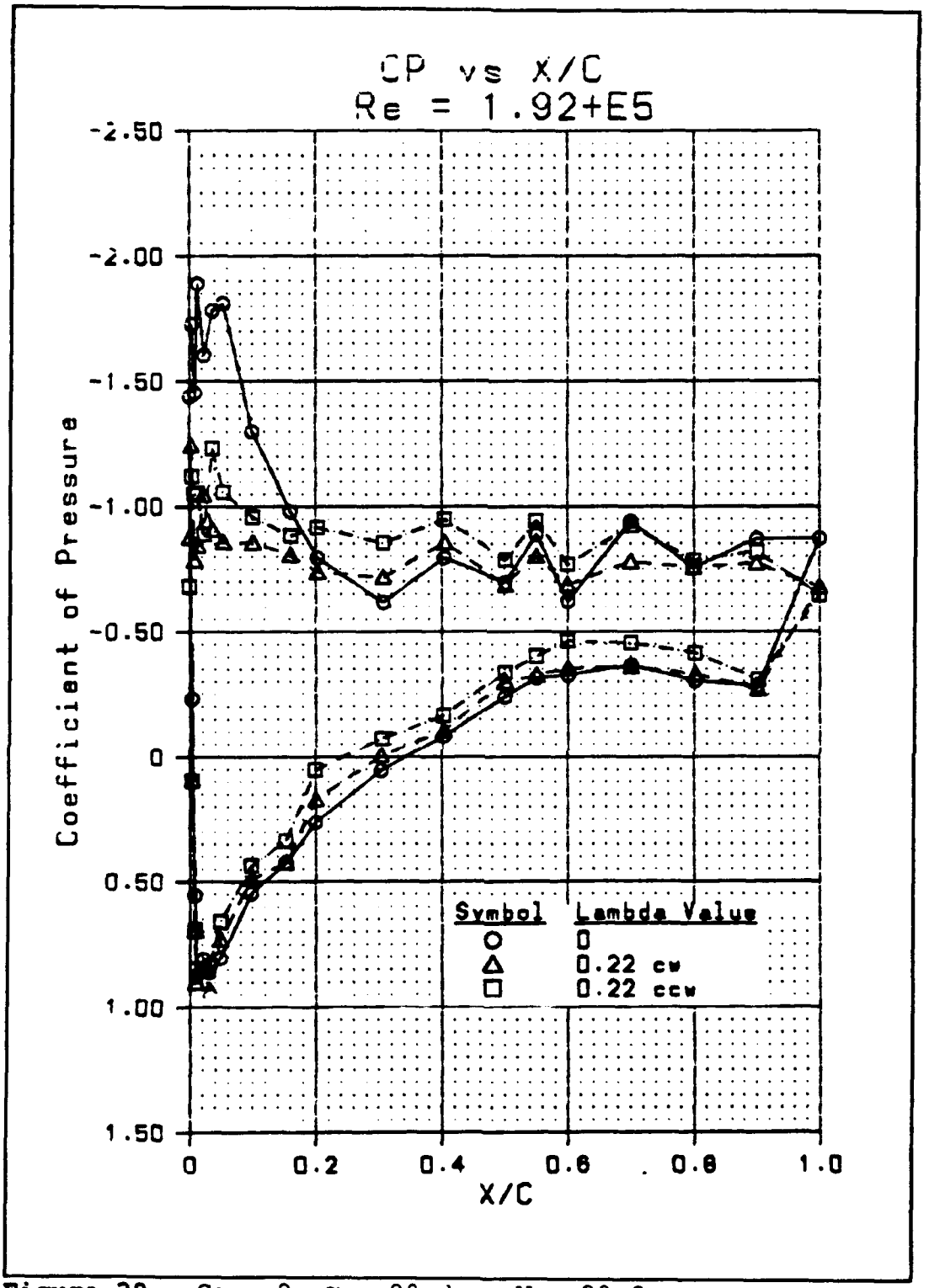

Figure 38. Case 2, α = 20 deg, V = 30 fps

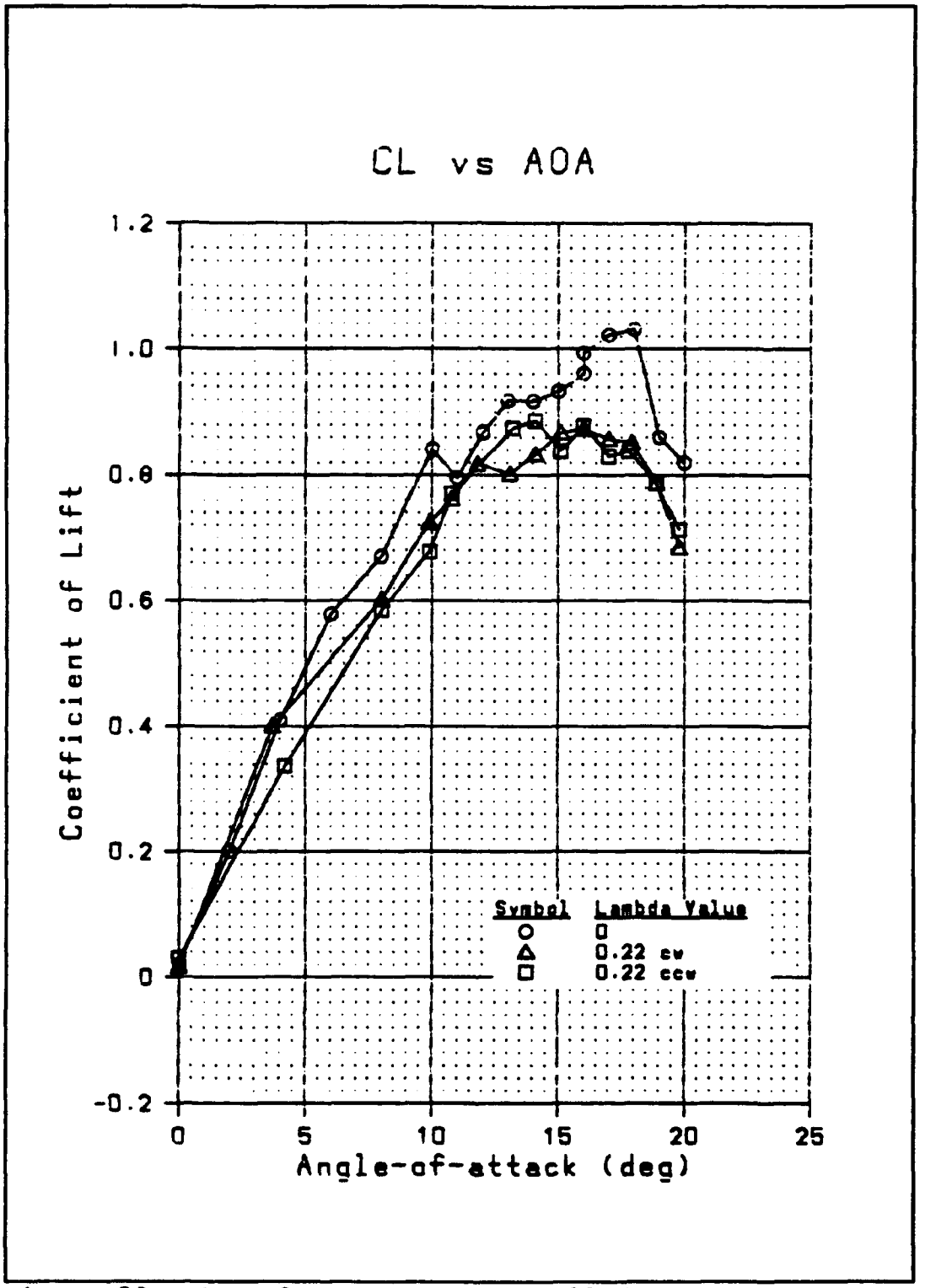

Figure 39. Case 2 Summary For V = 30 fps

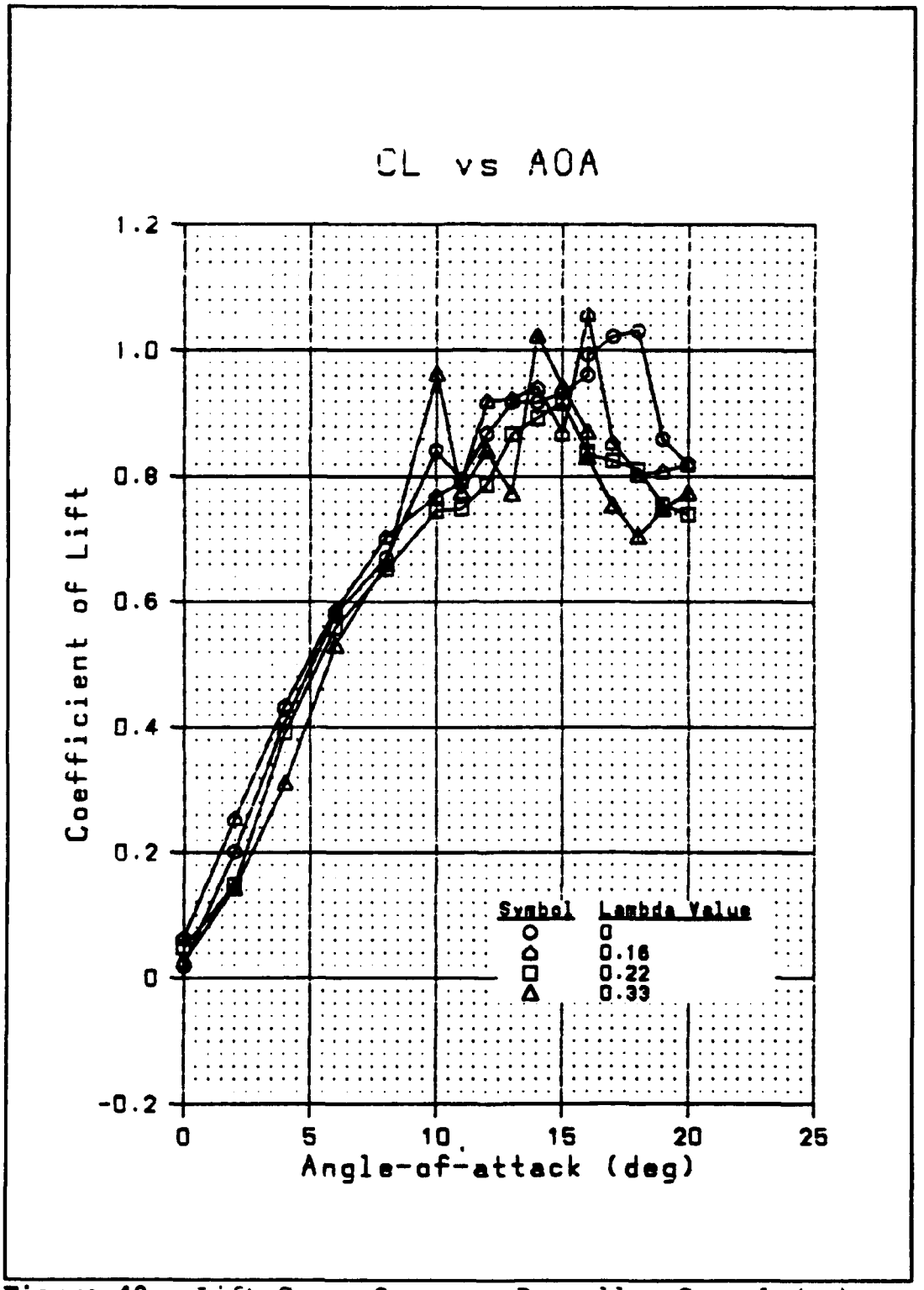

Figure 40. Lift Curve Summary, Propeller Case 1 (cw)

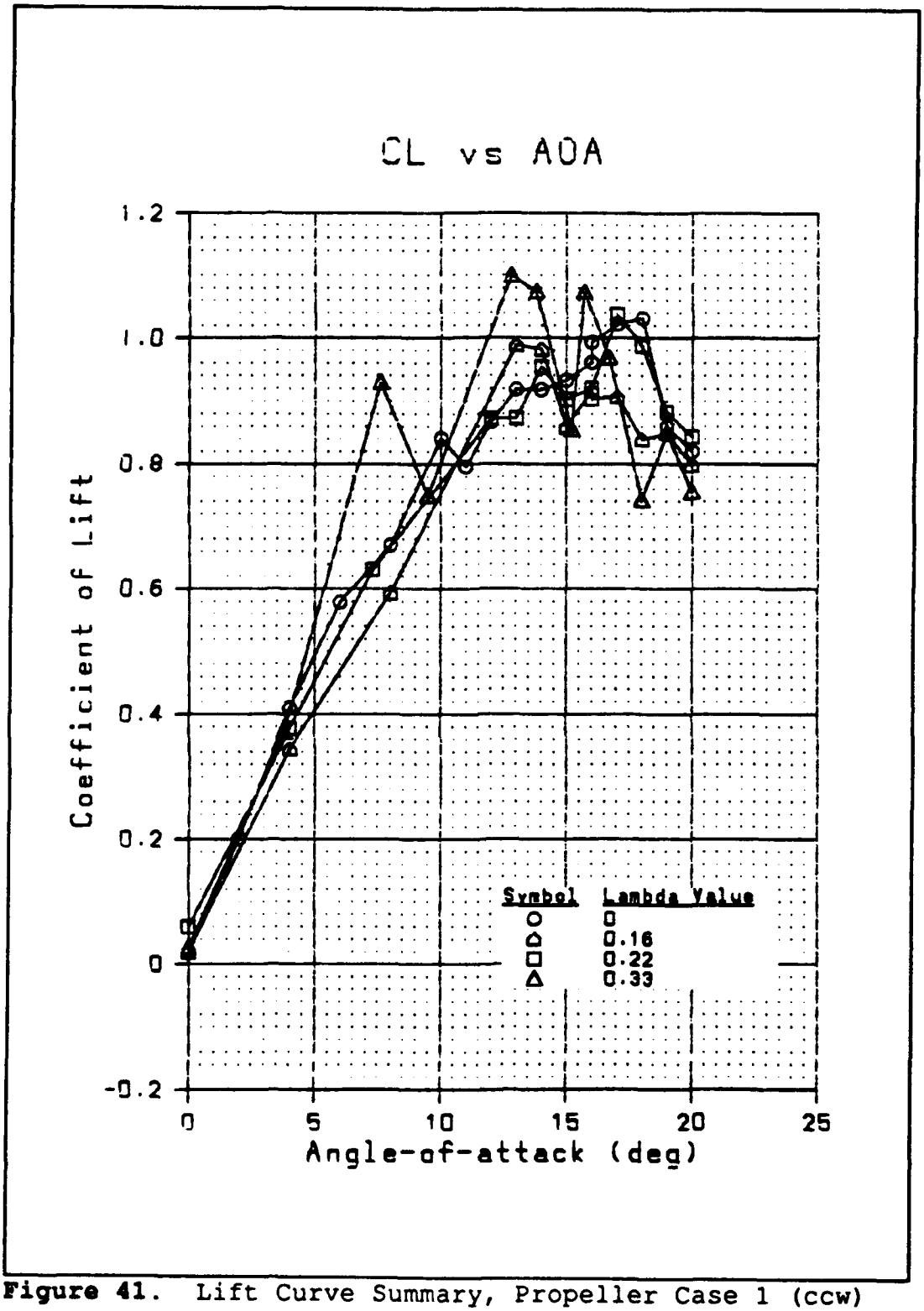

Figure 41. Lift Curve Summary, Propeller Case 1 (ccw)

LIST OF REFERENCES

1. Wu, J.Z., Vakili, A.D., and Wu, J.M., "Review Of The Physics OF Enhancing Vortex Lift By Unsteady Excitation," *Progress In Aerospace Sciences*, V. 20, No. 2, pp. 73-131, 1992.

2. Schmidt, Wilhelm., "Der Wellpropeller, Ein Neuer Antrieb Fur Wasser-, Land-, Und Luftfahrzeuge," *Z. Flugwiss*, 13(1965), Heft 12, pp. 472-479.

3. National Advisory Committee For Aeronautics Report 567, *Propulsion Of A Flapping And Oscillating Airfoil*, by I.E. Garrick, 4 May 1936.

4. *Laboratory Manual For Low Speed Wind Tunnel Testing*, Department of Aeronautics, Naval Postgraduate School, Monterey, California, October 1983.

5. Abbott, I.H., and Von Doenhoff, A.E., *Theory Of Wing Sections*, pp. 668-669, Dover, 1959.

6. DiMiceli, J.A., *Computer-Controlled Data Acquisition And Analysis*, Master's Thesis, Naval Postgraduate School, Monterey, California, September 1986.

INITIAL DISTRIBUTION LIST

1. Defense Technical Information Center 2
   Cameron Station
   Alexandria, Virginia 22304-6145

2. Superintendent 2
   Attn: Library, Code 1424
   Naval Postgraduate School
   Monterey, California 93943-5000

3. Chairman, Code AA/CO 1
   Naval Postgraduate School
   Monterey, California 93943-5000

4. Dr. M.F. Platzer 7
   Dept. of Aeronautics and Astronautics, Code AA/PL
   Naval Postgraduate School
   Monterey, California 93943-5000

5. Dr. S.K. Hebbar 2
   Dept. of Aeronautics and Astronautics, Code AA/HB
   Naval Postgraduate School
   Monterey, California 93943-5000

6. Mr. Carl W. Dane 1
   6510 Test Wing/EN
   Edwards AFB, California 93523-5000